Synthesis of Polyynes by Femtosecond and Nanosecond Laser Interaction with Matter

By

Sahr Al-Tuairqi

A thesis
presented to the University of Waterloo
in fulfillment of the
thesis requirement for the degree of
Master of Science
in
Physics

Waterloo, Ontario, Canada, 2018

Author's Declaration

This thesis consists of material all of which I authored or co-authored: see Statement of Contributions included in the thesis. This is a true copy of the thesis, including any required final revisions, as accepted by my examiners.

I understand that my thesis may be made electronically available to the public.

Statement of Contribution

HPLC data in this thesis was taken by Prof. Wakabayashi Tomonari of Kindai University. Polyyne purity in this thesis was calculated by Prof. Haruo Shiromaru of Tokyo Metropolitan University and his Master student Nobuyuki Takizawa.

None of these data has been published.

Abstract

A review of literature including some history and previous work done in the field is done showing the importance of polyynes themselves and as an important precursor in the formation of other interesting carbon nanoparticles for their own unique properties such as fullerene and carbon nanotubes. The review also shows some significant reseach papers connected to the experimental work done in this thesis.

Prior to the year of 1985, diamond, graphite, and amorphous carbon were the only 3 carbon allotropes known. In 1985 and while Harry Kroto and colleagues were working in their lab on an experiment involves laser ablation of graphite disc, a remarkably stable molecule that consists of 60 carbon atoms was detected, and was named later buckminsterfullerene. This discovery marked a watershed in the history of carbon allotropes raising a great scientific interest in carbon clusters and their production. Sumio Iijima was stimulated by this discovery to synthesize CNTs for the first time in 1991. MWCNTs are the second strongest material discovered after graphene, and SWCNTs have a thermal conductivity that is 3.5 times that of diamond, which is on the top of the thermal conductors list. Since then, many carbon allotropes have been discovered such as nanobuds and nanowires. Polyynes were reported later to be important precursors in the formation of fullerene and carbon nanotubes rising the interest in polyynes and polyynes productions.

Polyynes are one-dimensional hydrocarbon molecules consist of linear chain with even number of carbon atoms alternating single and triple sp-hybridized carbon bonds. Diacetylene is the simplest examples. Because of the high electron mobility in the carbon chains, polyynes have been used as nano-conductors and have been shown to form nanowires by inserting them into SWCNTs. Nanowires have unique properties that are different from the bulk materials. Polyynes have also been observed in nanostructured thin films production and were found to exist in the interstellar medium drawing astronomer's attention to them.

Femtosecond and nanosecond laser interaction with the matter in its liquid, gaseous and solid states to form polyynes is investigated through some polyyne synthesis experiments. The experiments that were done are laser irradiation of organic liquids, laser induced break down in hydrocarbon gases, and laser ablation of graphite. Experimental setup and procedures are demonstrated. UV-Vis spectroscopy, HPLC, and optical emission spectroscopy were used as the analytical techniques of polyynes produced in these experiments. Influence of the chosen targets on the products, the amount of polyynes produced and their purity from each method, irradiation time and pulse energy dependencies are discussed.

Acknowledgments

I would like to acknowledge my supervisor Dr. Joseph Sanderson for his insightful supervision and continuous discussions and guidelines, our collaborators Prof. Haruo Shiromaru and his group in TMU and Prof. Wakabayashi Tomonari and his group in Kindai University for their contribution in the experimental part of this project, the University of Waterloo people specially the Physics department members, my lab colleagues, the Saudi government for the generous scholarship, and finally my family for the endless support.

Dedication

To my parents, my husband and my siblings

Table of Contents

List of Tables

List of Figures

List of Abbreviations

RNA	Ribonucleic Acid
CNTs	Carbon Nanotubes
MWCNTs	Multi-Wall Carbon Nanotubes
SEM	Scanning Electron Microscope
SWCNTs	Single-Wall Carbon Nanotubes
HPLC	High Performance Liquid Chromatography
ISM	Interstellar Medium
DIBs	Diffuse Interstellar Bands
LIB	Laser Induced Breakdown
UV-Vis	Ultraviolet-Visible
HOMO	Highest Occupied Molecular Orbital
LUMO	Lowest Unoccupied Molecular Orbital
ODS	Octadecyl Silica
TMU	Tokyo Metropolitan University
SERS	Surface Enhanced Raman Spectroscopy

Chapter 1

Introduction

Nanotechnology is science, engineering, and technology conducted at the nanoscale (around 1 - 100 nm). Intensive studies are conducted in the field of nanotechnology working with nanoparticles. This was limited for centuries due to the unavailability of the proper techniques, but with the enormous developments of the analytical microscopies and spectroscopies, scientists have more knowledge of what they dealing with and more capable of studying and manipulating these nanoparticles. Special Ribonucleic Acid (RNA) strands that are attracted to cancer cells have been attached to nanoparticles filled with chemotherapy drug and used for drug delivery minimizing the terrible side effects of the drug. Water and stain repellent fabrics have been also made by the addition of nanoparticles with certain properties to the fabrics. Furthermore, many materials showed different and unique properties such as enormous strength when used in their nano sizes.

Carbon is one of the most interesting elements from a scientific point of view. Diamond, the hardest carbon allotrope, and graphite, one of the softest, with their unique properties such as good insulation and high conductivity, respectively, are two naturally

occurring carbon allotropes of interest. However, their bulk properties are what researchers have the most knowledge of. Since fullerene was discovered with its remarkable properties, nano-sized carbon clusters formation became a great scientific interest and studied extensively. In this work, polyynes, carbon clusters consisting of one dimensional chains, are the focus.

1.1 Research Objectives

- To gain sufficient knowledge and understanding of polyynnes and their importance and unique physical and chemical properties.
- To review previous work done in the field and to efficiently use what's been observed and reported to improve the results obtained in this work.
- To experimentally study and investigate the production of polyynes using different methods and comparing the results obtained from these methods and place some focus on the formation mechanism of polyynes.
- To apply analytical techniques for the identification and characterization of polyynes.

Chapter 2

Literature Review

2.1 Fullerene

Polyynes are reported to be important precursors in the formation of fullerene and carbon nanotubes [1-3]. Although carbon nanotubes (CNTs) are part of the fullerene family, the two terms are mentioned in the literature as separate structures. Mostly authors imply a specific structure from the fullerene family other than the carbon nanotubes when using the name fullerene. However, the importance of fullerene adds to the importance of polyynes, and, therefore, this section will be a review of some fullerene literature including some history and studies showing how significant the fullerene is in a way that aids the significance of polyynes. The term fullerene is a general term including any carbon only molecule that has a cage-like structure (hollow core), and the most popular two examples that can be given here are the spherical fullerene, a hollow sphere structure, which is called buckminsterfullerene, and the cylindrical fullerene, which is called carbon nanotubes. Fullerene exists also in many other forms such as ellipsoid and amorphous fullerene.

2.1.1 The Discovery of Fullerene

It was 1985 when Harry Kroto, James Heath, Sean O'Breie, Robert Curl and Richared Smalley were working in their lab at Rice University on an experiment to study the mechanism of long chain carbon molecule formation. The experiment involves an Nd:YAG laser, 30mJ pulse energy, irradiating a graphite disc to vaporize carbon clusters from the surface of the graphite disc to a high density helium flow and then detect them with time of flight mass spectroscopy. However, a very stable molecule that consists of 60 carbon atoms was detected. The structure of a truncated icosahedron, 12 pentagonal faces and 20 hexagonal, and 60 vertices, so that every atom of the C_{60} is placed at each vertex bonding with two other atoms with a single bond and double bond with the third, was suggested to explain such stability, see figure 2.1. The molecule was named buckminsterfullerene after Buckminster Fuller, an American architect, system theorist, designer, inventor, futurist and author, because of the many C_{60}-like geodesic dome structures designed by him [4]. Figure 2.2 shows one of his designs.

The molecule is also referred to as spherical fullerene and buckyballs. This discovery marked a watershed in the history of carbon allotropes raising a great scientific interest in the carbon cluster production in many areas. The discoverers won the Noble Prize in Chemistry in 1996 for this discovery. It's worth mentioning that the existence of buckminsterfullerene and its remarkable stability was predicted by Eiji Osawa, a Japanese professor, fifteen years earlier than the experimental discovery by Harry Kroto

[5, 6]. This theoretical study was not given enough attention until the discovery of fullerene by Harry Kroto.

2.1.2 Buckminsterfullerene Properties

Beside the buckminsterfullerene being extremely stable withstanding high temperature and high pressure, it is also the most symmetric molecule known having 3 types of symmetry axes [7, 8]. Buckminsterfullerene is an n-type semiconductor, but it becomes a conductor or superconductor when doped with alkali metals [5]. Potassium-doped C60 becomes a superconductor at 18K temperature [9, 10], and cesium-doped C60 becomes a superconductor at 38K under applied pressure [9].

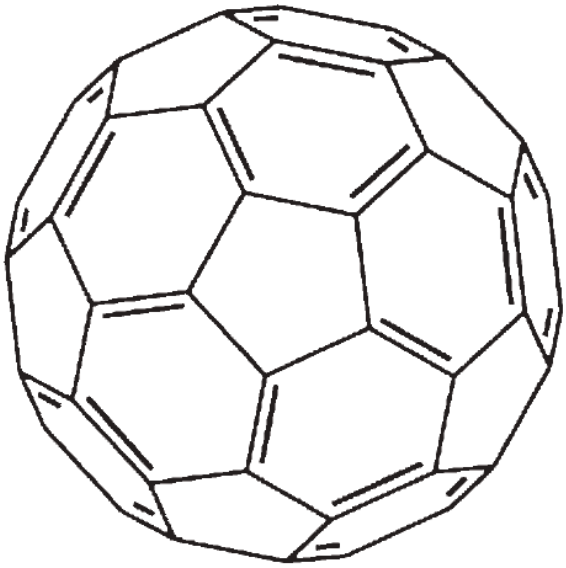

Figure 2.1. A molecular structure of buckminsterfullerene, C_{60}. [5] Reprinted with permission from Elsevier

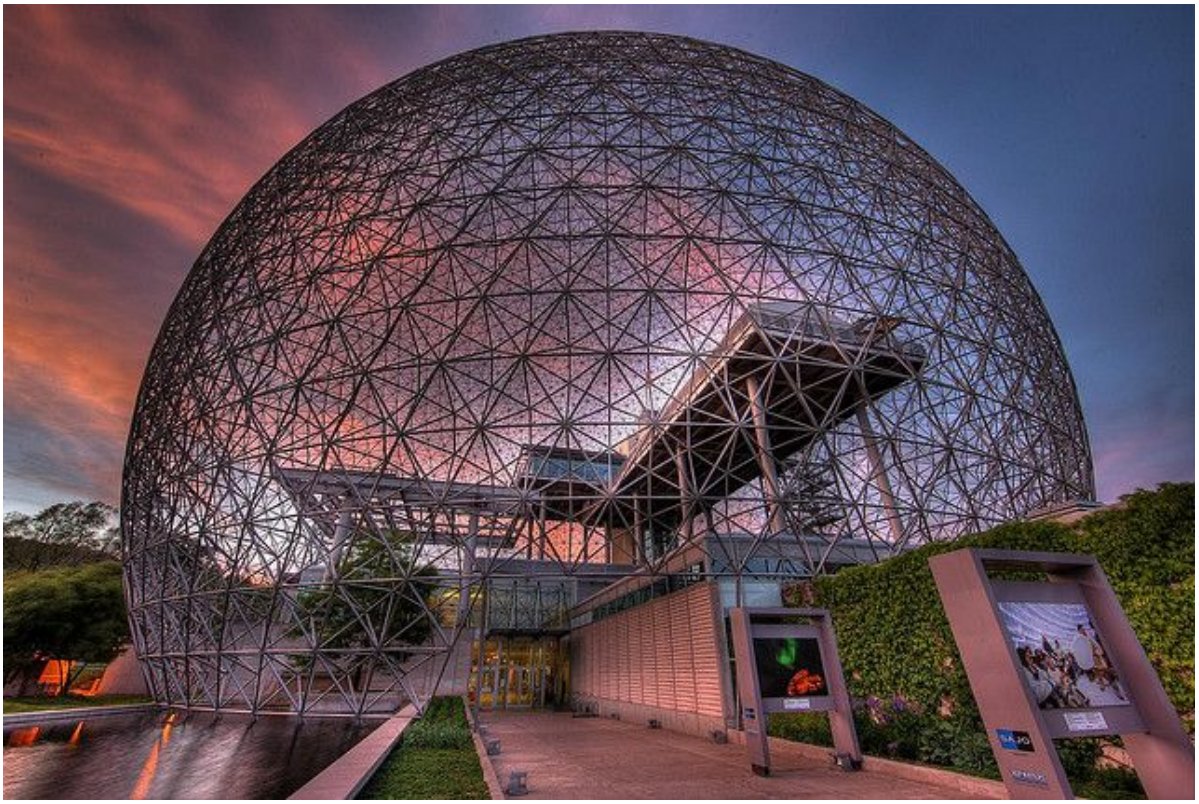

Figure 2.2. The Montreal Biosphère, a geodesic dome designed by Buckminster Fuller in 1967 in Montreal, Canada.

2.1.3 Carbon Nanotubes

Carbon nanotubes are hollow cylindrical nanostructures and can be also described as graphene sheets rolled up unto cylinders. In an experiment similar to the one used in reference [4], Sumio Iijima in 1991 was the first to synthesize carbon nanotubes, or the first to be credited for it. The experimental products were studied using a transmission electron microscope. Coaxial 2-50 walls nanotubes, multi-wall carbon nanotubes (MWCNTs), with various diameters and helical-like arrangements of the carbon atoms hexagons were observed. The micrographs shown in figure 2.3 illustrate three cases of the nanotubes produced [11].

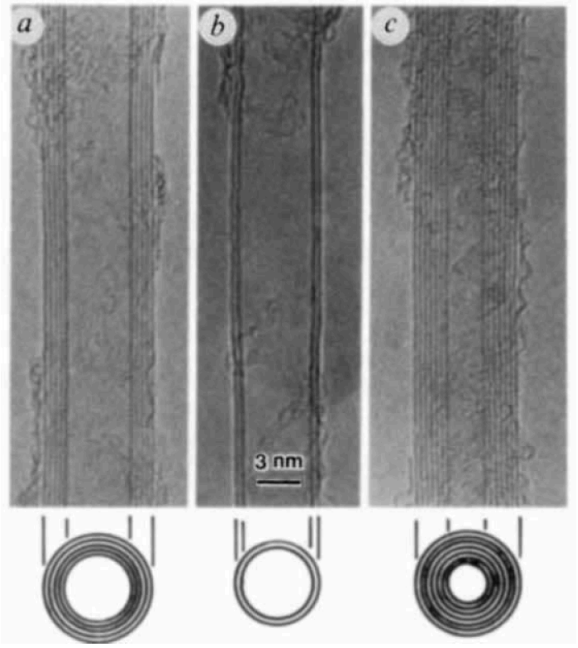

Figure 2.3. Electron micrographs of carbon nanotubes, A cross-section of each tube is illustrated: a. 5 graphene sheets with outside diameter OD = 6.7 nm, b. 2 graphene sheets, OD = 5.5 nm, c. 7 graphene sheets, OD = 6.5 nm, and smallest inside diameter ID = 2.2 nm. [11] Reprinted with permission from Springer Nature

The properties of carbon nanotubes differ depending on the number of walls, the inner and outer diameter, and the arrangement of carbon atoms and hexagons, which can be thought of as the angle that the graphene sheet folded at. Despite of these differences, carbon nanotubes all have unusual mechanical, thermal, chemical, electrical and optical properties.

The tensile strength is defined as the maximum stress a material or structure, being pulled apart, can take before it fails or breaks. MWCNTs were examined using scanning electron microscope (SEM) in terms of their tensile strength. The maximum stress the outer tube of the MWCNTs withstand before breaking was 63 Gigapascals (GPa)[12]. The theoretical number is even much higher. It was calculated to be 300 GPa [12, 13, 14]. This makes carbon nanotubes the second strongest material discovered after graphene since graphene was tested to have 130 GPa tensile strength with a theoretical computation of 1 TPa [15]. The highest measured tensile strength of maraging steel is 3.5 GPa, where maraging steel is an alloy of iron strengthened by adding some other metals like nickel and cobalt in specific percentages depending on the properties needed.

On the top of the thermal conductors list, there is diamond, silver and copper. These good conductors have a thermal conductivity of 1000 W/m.K (watts per meter-kelvin), 406 W/m.K and 401 W/m.K respectively at room temperature. However, Pop et al. (2006) studied the thermal conductivity of single-wall carbon nanotubes (SWCNTs)

that have a 2.6 μm length and 1.7 nm diameter at temperatures ranging from 300-800 K, and they were found to have a thermal conductivity equals to 3500 W/m.K at room temperature along the tubes' axes[16], which is 3.5 times that of diamond. Furthermore, depending on how the graphene sheets are rolled up into the nanotubes, nanotubes can be metallic, quasi-metallic or semiconductors also along their axes. As a result, carbon nanotubes have been used or proposed for applications where such unique thermal and electrical properties are desired such as transistors and interconnects in integrated circuits [16, 17-19] and thermal interface materials in thermal management [16, 20].

2.1.4 Polyynes Encapsulated in Carbon Nanotubes to form Nanowires

Carbon nanotubes are hollow cylinders, while nanowires have a solid cylindrical structure, both with extreme slenderness. Because of their extreme slenderness, two of their three dimensions are between 1-100 nanometers, and the third dimension is the only dimension the electrons propagate along, nanowires just like nanotubes are considered one dimensional materials with exceptional properties. Nanowires also can be defect-free due to their tremendously small and very simple structure. CNTs have been used or reported to encapsulate polyynes [21], fullerenes [22-24], metallofullerenes [25-27], water molecules [28], organic compounds [29, 30], and metal complexes [31] forming hybrid materials called peapods for a variety of purposes in different industrial and scientific fields.

In a study done in 2006, n-hexane with suspended graphite particles was irradiated with Nd:YAG laser, 532 nm, 10 Hz, 100 mJ/pulse, 10 mm spot size, for one hour to synthesize polyynes. The irradiated sample was then filtered to remove the residual particles formed. $C_{10}H_2$ was separated from the other polyyne chains synthesized, C_8H_2 and $C_{12}H_2$, and purified using High Performance Liquid Chromatography (HPLC). M-containing carbon was heated to 1250 °C and then irradiated with 350 mJ/ pulse, 6 mm spot size, for 3 hours (a high temperature laser ablation method) to synthesize SWCNTs. A rinse with toluene and a treatment with H_2O_2 and HCl aqueous were then employed to remove the co-existing fullerene, amorphous carbon and metal particles. The purified SWCNTs in the film-like material was heated in dry air at 500°C for 30 min. A glass ampoule of a Y-branched shape with one end filled with the $C_{10}H_2$ Solution and the SWNTs in the thin film placed at the other end was used to synthesize a $C_{10}H_2$@SWCNTs hybrid ($C_{10}H_2$ polyyne inside SWCNTs). The ampoule was evacuated and then the $C_{10}H_2$ Solution and the SWNTs in the thin film were mixed. The $C_{10}H_2$@SWNTs hybrid was characterized by Raman spectrometer (figure 2.4) showing signal at 2066 cm^{-1}. The hybrid was heated for different temperatures from 150-500 °C to study the thermal behavior, and it was stable until above 300 °C, and then the signal started to decrease. $C_{10}H_2$ staying stable until above 300 °C is impressive especially with a molecule that is highly reactive [21].

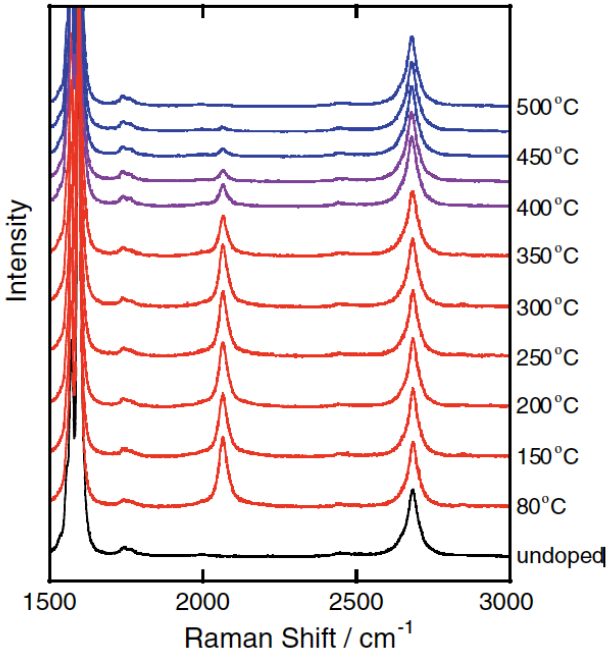

Figure 2.4. Temperature-dependence of Raman spectra of undoped SWCNTs and C10H2-doped SWNTs. [21] Reprinted with permission from Elsevier

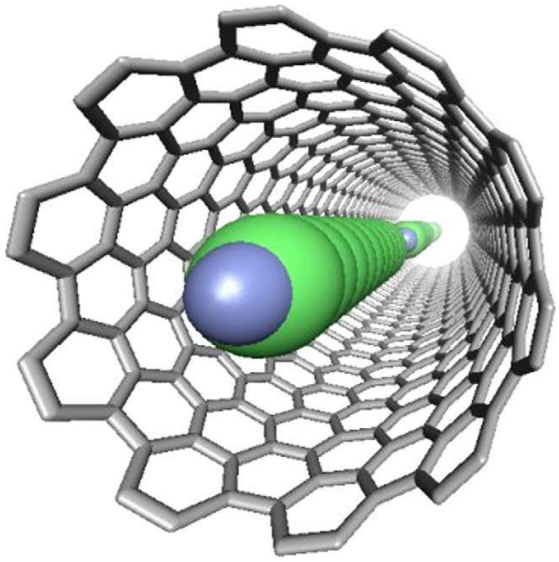

Figure 2.5. A schematic drawing of The polyyne $C_{10}H_2$ peapod inside the SWCNTs. [21] Reprinted with permission from Elsevier

2.2 Polyynes

Polyynes $(-C\equiv C-)_n$ (n >1) are hydrocarbon molecules which consist of a linear chain of an even number of carbon atoms alternating single and triple sp-hybridized carbon bonds. They are one-dimensional materials. and are rigid compared to the other organic compounds. Diacetylene C4H2 ($H-C\equiv C-C\equiv C-H$) is the simplest polyyne molecule, and Carbyne $(-C\equiv C-)_\infty$ is the theoretical infinite polyyne. Polyynes are end-capped with an atom or group of atoms that is usually hydrogen, but can be methyl group (CH3), ethyl group (CH2CH3) or many other groups. The hydrocarbon molecules that consist of carbon atoms in a chain but with double bonds between them are different from polyynes and called cumulenes. Butatriene ($H_2C=C=C=CH_2$) is the simplest example of cumulenes. Polyynes are also distinguished from the polyacetylene $(C2H2)_n$ that is obtained by the polymerization of acetylene molecule. Long chain polyynes are reported to be unstable since they can cross-link with each other and explode [32], but they can be stabilized with a proper bulky end-cap such as tert-butyl and trifluoromethyl [33, 34].

In addition to polyynes being an important precursor in the formation of fullerenes and carbon nanotubes, and being used as nanowires by inserting them in SWCNTs, they have been used as nano-conductors due to the high mobility of electrons in the polyyne chains [35], and have been observed in the production of nanostructured

thin films [35, 36]. Carbyne $(-C\equiv C-)_\infty$ was theoretically predicted to be stable at room temperature with double the tensile strength of graphene, and when end-capped with CH2 groups, it could obtain a nonzero stiffness and if also twisted by 90°, it could switch into a magnetic semiconductor state [37, 38].

2.2.1 Polyynes in astrophysics

The interstellar medium (ISM), in astronomy, is the matter and radiation that fills the space between the star systems in a galaxy. It was commonly believed that the space between the stars is a complete vacuum (no existance of any material) until the observation of dark areas that looked like holes in space in the photographs taking by telescopes in 1904. These dark areas were revealed later on to be interstellar clouds blocking the stars behind them. An interstellar cloud is defined as an accumulation of gas, plasma and dust, and it is denser than average regions of the interstellar medium. Astronomers' attention was drawn to polyynes since they were found to exist in the interstellar medium [35, 39-41]. The centrosymmetric C3 molecule (a carbon chain) was detected by its far IR bending rotation transitions in a cold (10-30 K) interstellar dust cloud [40, 42]. ζ Ophiuchi is a star in the constellation of Ophiuchus, the third brightest star in the constellation. Diffuse interstellar bands (DIBs) of hydrogen containing polar chain molecules were observed near this star, and after further laboratory studies, it was found that long carbon chains such as HC_nH, C_{2n}, C_nH, HC_nH^+, and C_n^- are potentially in these DIBs [40, 43], which indicates the potential of polyynes existence in these DIBs.

2.3 Polyyne Synthesis

At first, polyynes were produced using traditional chemical (organic synthetic) methods, and long polyynes up to n=22 were reported to be synthesized using an oxidative coupling method [35, 44, 45]. However, these chemical methods are not the best approach to produce polyynes because of the risk factor involved. As mentioned previously, uncapped polyynes are highly reactive molecules, and using such techniques could lead to an explosion.

Laser based methods were first used in 1985 by Rohlfing et al. [46, 47], and recently have been employed intensively to synthesize polyynes in the liquid and gas phases in various ways. Carbon particles such as graphite, fullerene, or nano-diamond were suspended in organic liquids and then irradiated by a ns laser. Polyynes up to n=15 were reported from this method [48, 49]. Without the need for the introduction of carbon particles, polyynes were synthesized by fs laser irradiation of organic liquids [35, 37]. Polyynes with much higher purity than those made in liquid solution were produced by ns laser ablation of graphite in a gas mixture flow and from ns and fs laser induced breakdown (LIB) in gaseous hydrocarbons prepared either by bubbling argon in organic liquids or using hydrocarbon gases directly [46, 53]. Those obtained from fs laser ablation or induction have higher polyyne purity.

More detailed reviews of some of the most significant polyyne production research papers that are connected directly to the experimental work done for this thesis are provided next.

2.3.1 Liquid Irradiation of hydrocarbons with suspended graphite particles

In a research paper studying the production of hydrogen-capped polyynes in liquids, two Nd:YAG lasers one with 355 nm and 532 nm and the other 1064 nm wavelengths, 10Hz repetition rate, 5-9 ns and 1μs, respectively, pulse duration were used to irradiate benzene, toluene and hexane solutions with Graphite particles suspended in them. The laser was either focused using a lens with f=100mm or not focused. The samples were irradiated for one hour, filtered, and then analyzed using HPLC coupled with a UV-Vis spectrometer and GC/MS. The best HPLC spectra of the three solutions were chosen at the highest absorption. Benzene and toluene spectra were similar, whereas the toluene and hexane peak numbers and intensities were different. C8H2 was observed in hexane but not in toluene, C16H2 was observed in toluene but not in hexane, and C10H2, C12H2, C14H2 were observed in both. The HPLC and UV spectra are shown in figure 2.6 and figure 2.7. The positions of the observed peaks correspond to the peak positions of previously reported hydrogen-capped polyynes by another research group [44]. Results from focused and unfocused lasers were similar. However, the results show that the absorbance and the formation rates decrease as the wavelength increases, and increase as the graphite particle concentration increases from 0.5-4mg/ml and then decrease from 4-10mg/ml [49]. Peaks positions from [44] and [49] are summarized in table 2.1.

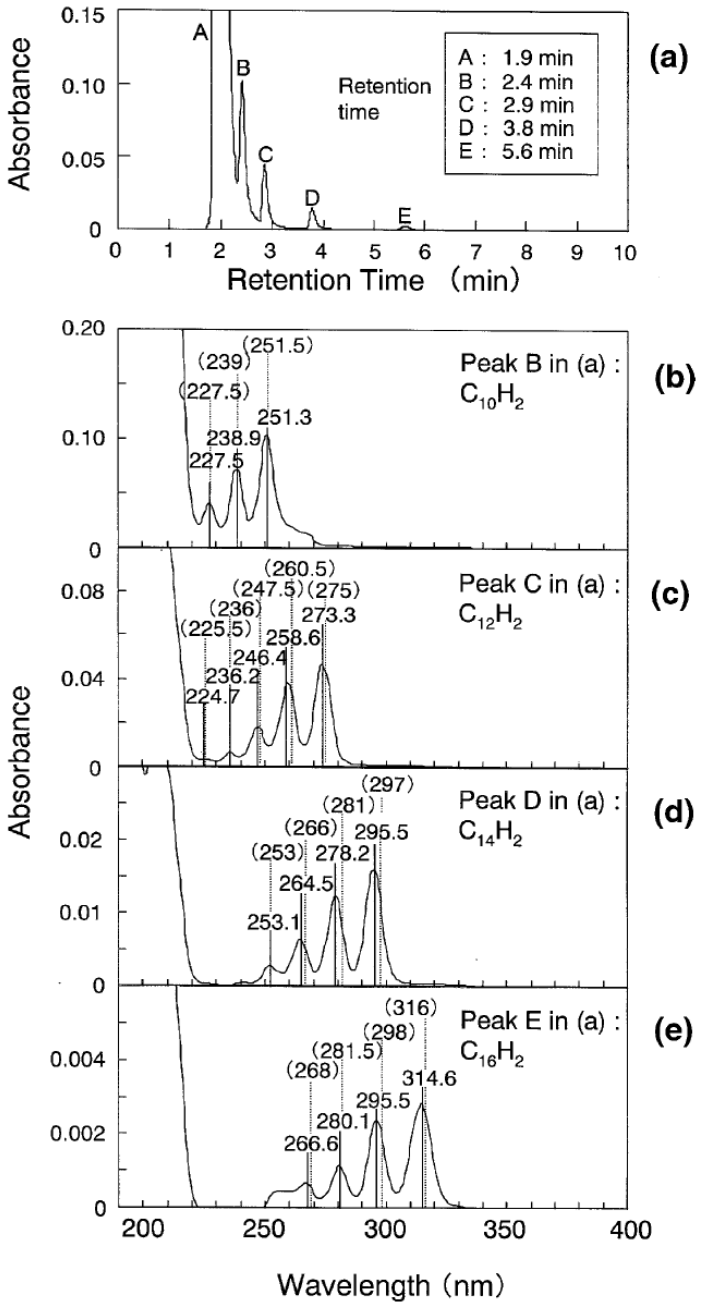

Figure 2.6. (a) HPLC spectrum and (b–e) UV spectra of products resulting from unfocused 355 nm laser irradiation on graphite particles suspended in toluene solution at room temperature. Values in parentheses on the UV absorption peaks are reported in [44]. [49] Reprinted with permission from Elsevier

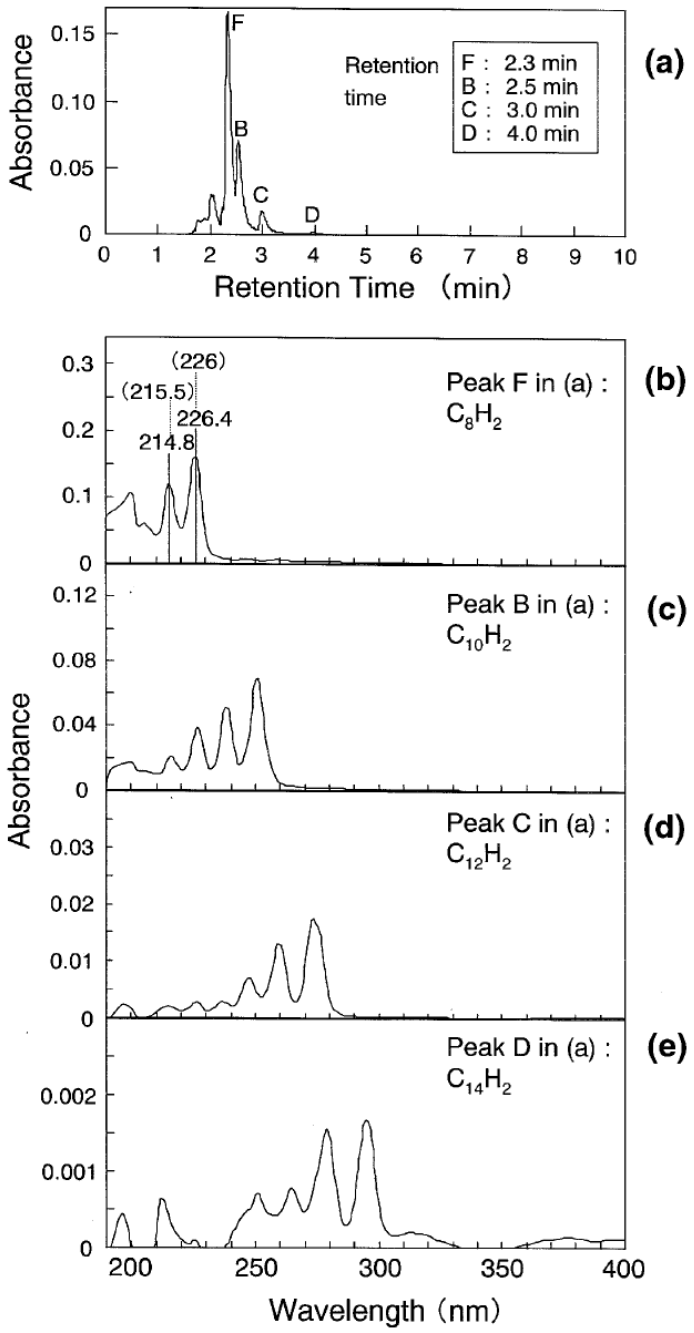

Figure 2.7. (a) HPLC spectrum and (b–e) UV spectra of products resulting from unfocused 355 nm laser irradiation of graphite particles suspended in hexane solution at room temperature. Values in parentheses on the UV absorption peaks are reported in [44]. [49] Reprinted with permission from Elsevier

	Polyynes peaks' position (nm)	
	[44]	[49]
C8H2	215.5 , 226	214.8 , 226.4
C10H2	227.5 , 239 , 251.5	227.5 , 238.9 , 251.3
C12H2	225.5 , 236 , 247.5 , 260.5 , 275	224.7 , 236.2 , 246.4 , 258.6 , 273.3
C14H2	253 , 266 , 281 , 297	253.1 , 264.5 , 278.2 , 295.5
C16H2	268 , 281.5 , 298 , 316	266.6 , 280.1 , 295.5 , 314.6

Table 2.1. Summary of polyyne peak positions reported from [44] and [49].

2.3.2 Liquid Irradiation of organic liquids without the introduction of carbon particles

In their paper "Synthesis of polyyne molecules from hexane by irradiation of intense femtosecond laser pulses", researchers irradiated n-hexane liquid, with 79% purity, to form polyynes with different chain lengths using an amplified Ti:Sappire laser with 800nm wavelength, 100fs pulse duration and 1kHz repetition rate. The laser was focused using a 5cm focal length lens forming a bright filament with 4×10^{13} W/cm^2 intensity in the target. Polyynes were formed after irradiation of the target for 30-300 min, and no change in the color or formation of carbon precipitate was observed. The sample was analyzed with standard UV-Vis spectroscopy using pure hexane as a reference, and then polyynes were separated using HPLC for more detailed analysis (figure 2.8). Later, resonance Raman spectroscopy was employed to confirm the presence

of polyynes. Polyynes from C6H2 to C12H2 were detected although part of C6H2 was believed to be evaporated because of the high vapor pressure. When using higher pulse power, the signal intensity was increased but with the same polyyne ratios indicating no change in peak intensity but a larger interaction volume [35].

In another research paper studying the production of hydrogen- and methyl-capped polyynes in liquids, published in 2017, an amplified Ti:Sapphire laser with 800 nm central wavelength, 1kHz repetition rate, 35fs pulse duration and 300 μJ pulse energy was used to irradiate toluene, with 99.9% purity, without the introduction of any carbon particles. The laser was focused using a biconvex lens with f=50mm at the meniscus of the samples. The samples were irradiated for 1- 4 hours. A gradual change from colorless to dark yellow, and formation of black precipitate were observed during the experiment. To confirm the presence of polyynes, Raman spectroscopy was used, and then HPLC coupled with a UV-Vis spectrometer was used to characterize and distinguish the polyynes formed in the irradiated samples (see figure 2.9 for the UV-Vis and HPLC data). Samples irradiated for 3 and 4 hours showed sufficient concentration of polyynes. Hydrogen-capped polyynes from C12H2 to C18H2 were observed. Methyl-capped polyynes HC12CH3 and HC14CH3 in the sample irradiated for 3 hours corresponded to previously reported methyl-capped polyynes. Selecting the organic liquid used in the irradiation could be a way to control the end-caps of polyynes produced [37]. This work was done in our femtosecond laser laboratory located at the Physics and Astronomy Department in the University of Waterloo.

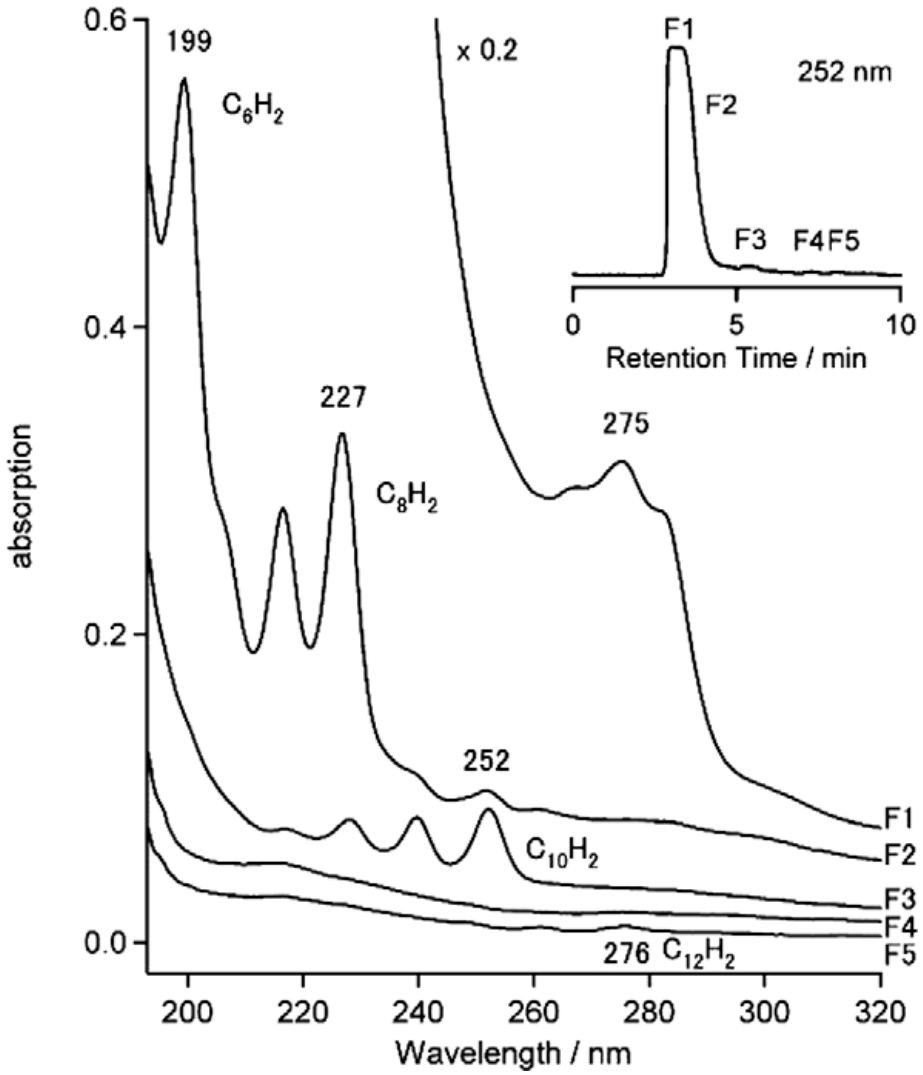

Figure 2.8. Absorption spectrum of each the fraction, F1–F5, indicated in the inserted preparative HPLC chart of the sample irradiated 3 h with the power 0.90 mJ/ pulse. [35] Reprinted with permission from Elsevier

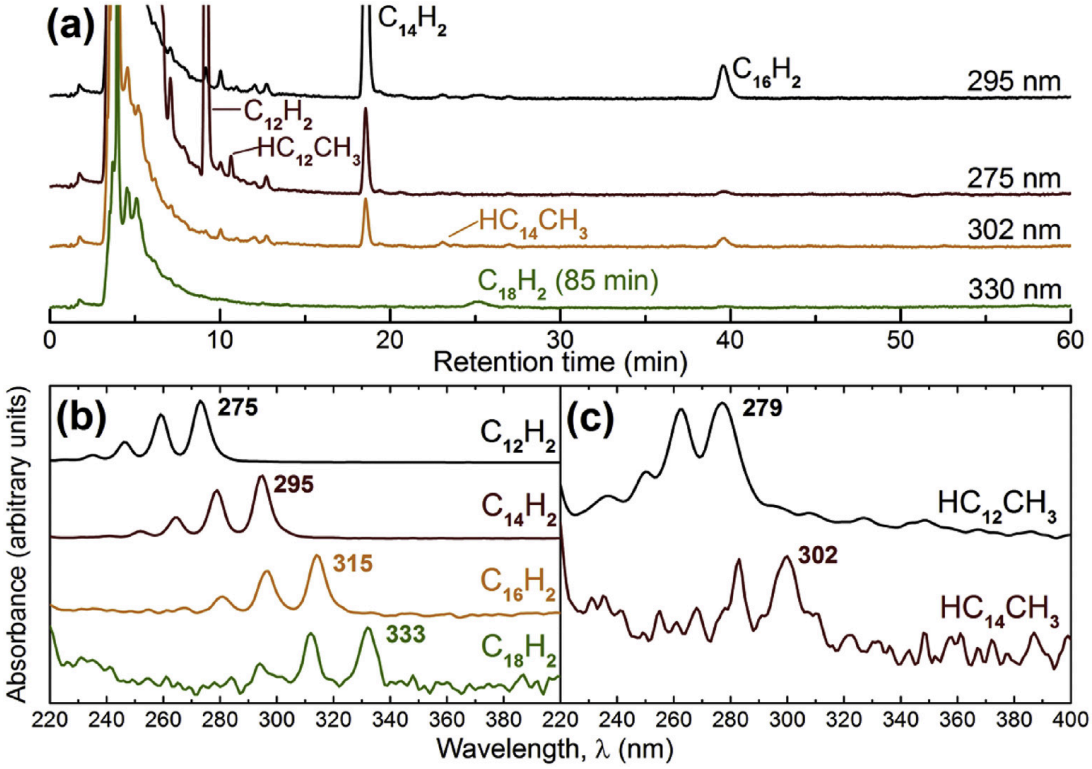

Figure 2.9. (a) HPLC chromatograms taken at various absorption wavelengths. Peaks corresponding to each polyyne are labeled. The C18H2 peak shows up one analytical cycle later at 85 min. The wavelengths were chosen to showcase all possible synthesis products using the minimum number of curves. (b) UV-Vis absorption spectra of individual hydrogencapped polyynes, H(C≡C)nH (n = 6-9), from separated fractions extracted through HPLC with the maximum absorption peaks labeled in nanometers. Each absorption spectrum is normalized such that the baseline (zero absorbance) is at zero while the maximum value is 1. The spectra are offset for clarity. (c) Same as (b) but for methyl-capped polyyne fractions, H(C≡C)nCH3 (n = 6,7). These spectra were extracted for a sample irradiated for 3 hours. [37] Reprinted with permission from Elsevier

2.3.3 Gas Phase (Bubbling Argon in organic liquids) or (Directly from hydrocarbon gases)

In 2017, [53] carried out ns and fs Laser Induced Breakdown experiments on propane, hexane, octane, benzene and toluene. The ns laser used was an Nd:YAG laser with 532 nm wavelength and 30 Hz repetition rate, focused with a 70 mm lens at the center of the irradiation cell, producing energy of 150mJ/pulse. Targets were irradiated for 60 seconds. The fs laser used was an amplified Ti:Sapphire laser with 800 nm wavelength and 1 KHz repetition rate, focused at the center of the irradiation cell with an 80 mm lens, producing energy of 1.5 mJ/pulse. Hexane was irradiated for 5 minutes, and toluene for 10 minutes. The propane gas was mixed with argon and the propane ratio, $R = f_p/(f_p + f_a)$, $f_p + f_a = 50\ mL/min$, dependency was investigated, where f_p and f_a are the flow rates of propane and argon. Argon was bubbled into hexane, octane, benzene and toluene to form gaseous mixtures with flow rate of 50 mL/min. The experiments' products were dissolved in cooled hexane. To ensure a contamination-free irradiation cell, the hexane was kept at $-80°C$ preventing evaporation into the target area, and the flow rate was kept at 50 mL/min. Plasma was formed around the focus spot during the irradiation, and the emission was characterized using a fiber spectrometer. Another ns laser with 1064 nm wavelength (460 mJ/pulse) was used to observe the overall spectral features of the emission. The fiber spectrometer range was from 400 – 800 nm, and that's why a different laser was used, so that the peak from the laser will not be presented in the emission spectra. The samples resulted were filtered and then a UV spectrometer was employed to identify the formed polyynes. H-capped polyynes with high purity

(maximum $\chi_p \cong 0.25$) were produced from the ns LIB. Polyyne purity will be explained more in section 3.2. The propane absorption data showed propane ratio dependency, where absorbance, amount of polyynes produced, increases with increased R, whereas, the purity of the polyynes produced was found to be independent of the ratio of propane. The polyynes yield and purity of polyynes as a function of R are plotted in figure 2.10. The emission spectra of the formed plasma from the LIB with 1064 nm and 532 nm ns lasers are shown in figure 2.11. Swan bands were observed in these spectra indicating the existence of the radical diatomic carbon C2, which is an indication of a sufficient formation of carbon clusters. This observation supports the polyynes formation mechanism of ethynyl radicals (C2H) interaction with unsaturated hydrocarbons [50, 51], and the polyynes production reaction ($C_2H + CH_3C{\equiv}CH \rightarrow C_4H_2 + CH_3$) reported by [52]. No observation of the swan band in the argon/toluene spectrum indicates low formation of C2, which correspond to the lower polyyne yield from the sample. H-capped polyyens were synthesized from the fs LIB with lower yield of C6H2 and C8H2, but with much higher polyyne purity ($\chi_p \cong 0.46$) [53].

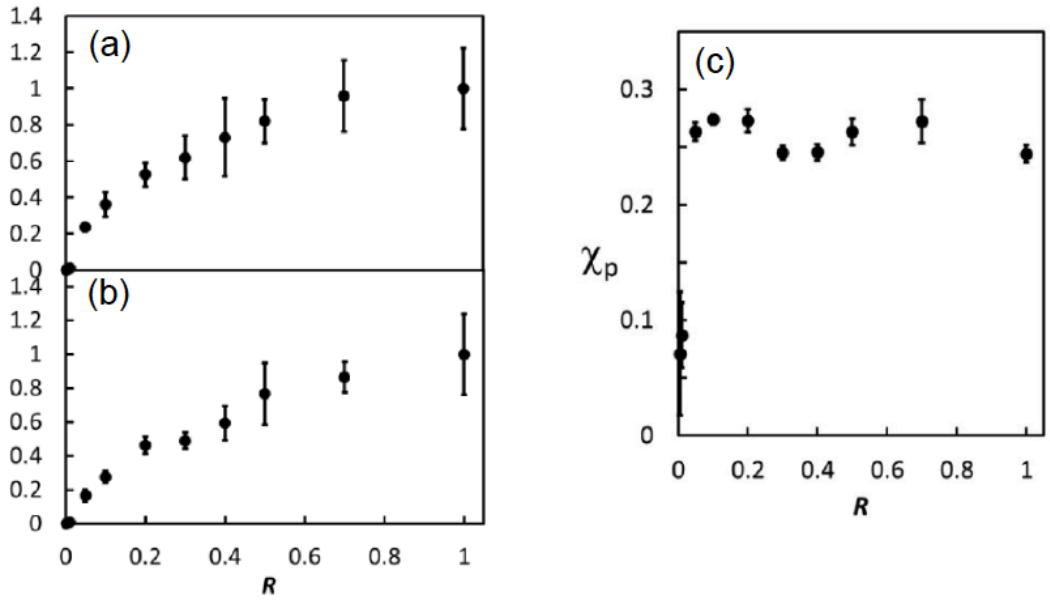

Figure 2.10. The estimated polyyne yield in the product solution obtained by ns-LIB of propane/Ar gas flow. (a) Plot of the yields versus R for C6H2, (b) that for C8H2. The yields are normalized at R =1. (c) Plot of χ_p versus R. [53] Reprinted with permission from Elsevier

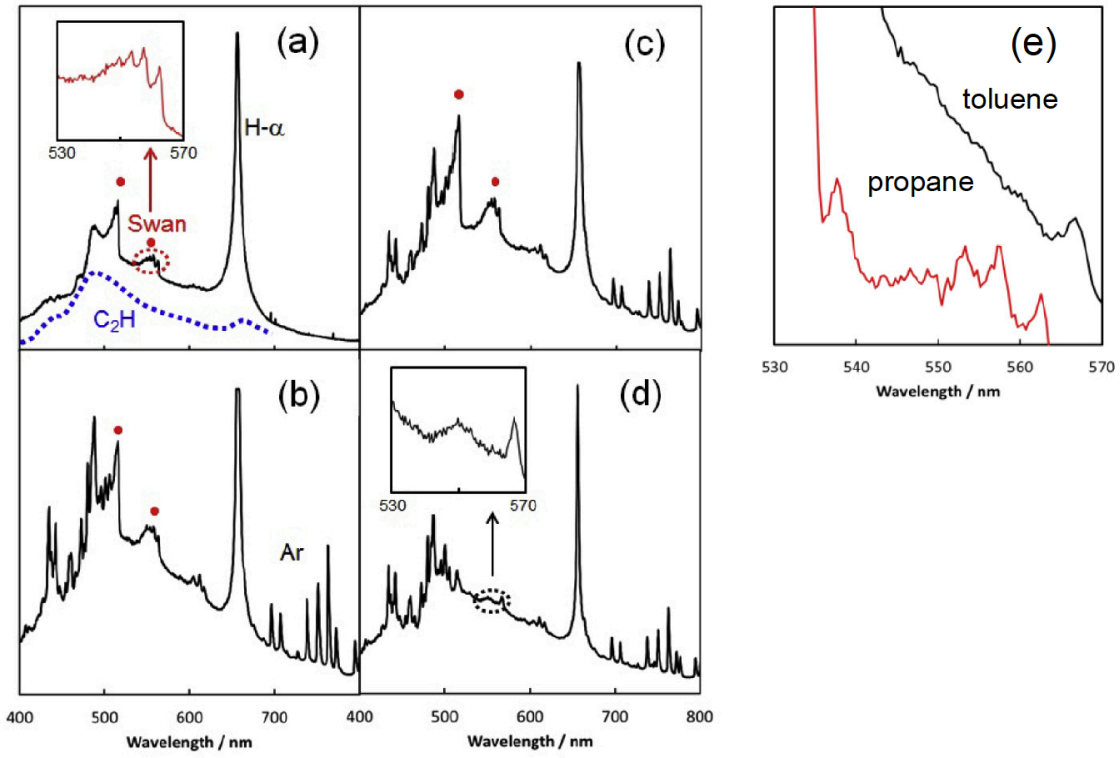

Figure 2.11. (a) Emission spectrum of the 1064-nm-ns-LIB in propane (black). The Swan band is indicated by the red filled circles, and that around 550 nm in an expanded scale is shown in the inset. Emission spectrum of C2H, a tracing of the spectrum in [35], is shown as the blue dashed curve. (b) Emission spectrum of the 1064-nm-ns-LIB in octane/Ar. (c) Emission spectrum of the 1064-nm-ns-LIB in benzene/Ar. (d) Emission spectrum of the 1064-nm-ns-LIB in toluene/Ar. The inset shows the spectrum in an expanded scale around 550 nm. (e) Emission spectra of the 532-nm-ns-LIB in propane (red) and in Ar/toluene (black). [53] Reprinted with permission from Elsevier

2.3.4 Graphite Ablation in Hydrocarbon Gas Flow

In a similar setup to the one used in the LIB experiments, the synthesis of polyynes by laser ablation of graphite is investigated by placing, in the irradiation cell, a graphite disc with many small through-holes (1mm) to allow the gas to flow through. Argon/propane mixture is prepared with propane ratio R and flow rate fixed at 50 mL/min and ejected in the direction to the cooled hexane prepared to capture the product polyynes, so that the polyynes formed on the surface of the graphite disc are carried to the hexane. Nd:YAG laser with 532 nm wavelength and 30 Hz repetition rate that produces average energy of 150 mJ/pulse is focused behind the graphite disc forming an interaction area on the graphite surface of 30 mm^2. The irradiation continues for 60 seconds. The products and the propane gas are condensed into the cooled hexane, and then the propane evaporates when the sample is heated to room temperature. Using the same laser parameters, suspended graphite particles in hexane are ablated for comparison. Samples were filtered and then diagnosed with a UV-Vis spectrometer. A significant difference is shown in the absorption spectra in term of polyyne size distribution, and higher absorbance is observed with increased propane ratio R (see figure 2.12). Moreover, a much lower amount of unresolved hydrocarbons are formed in the case of laser ablation in the gas phase. The methylpolyynes $H(C_{14})CH_3$ and $H(C_{16})CH_3$ are also formed in the gas phase case with peak positions at 303 nm and 325 nm, respectively. Their peak positions correspond the methylpolyynes' peak positions estimated by [54]. The yield of each H-capped polyyne (n=3-7) as a function of the propane ratio R is plotted to confirm the R-dependency (figure 2.13) [46].

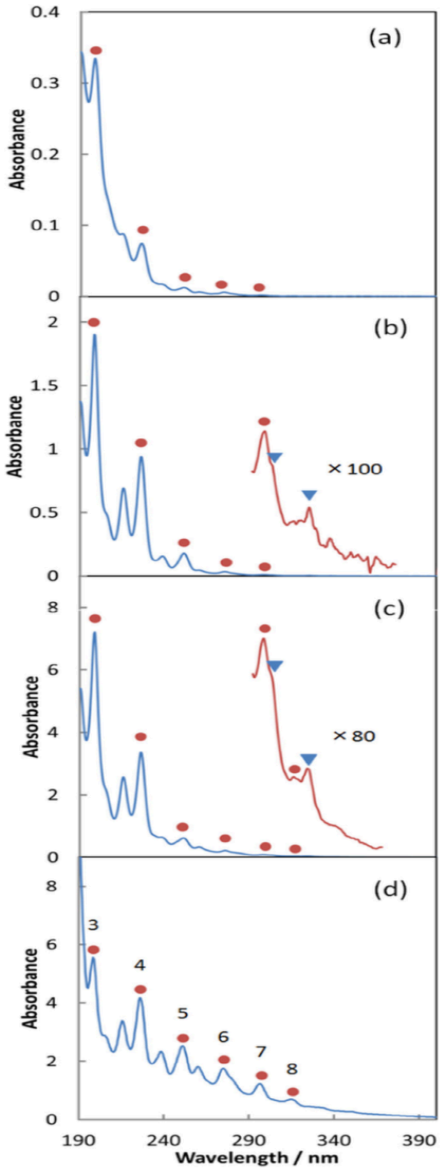

Figure 2.12. Absorption spectra of the solutions prepared by laser ablation of graphite in (a) argon (R=0), (b) 5% propane (R = 0.05), (c) 100% propane (R = 1), and (d) in hexane solution. The 0–0 vibrational bands of the polyynes are indicated by the filled circle, and in (d) with the numbers n of $C_{2n}H_2$. The triangles in the magnified plots indicate the 0–0 bands of methylpolyynes, H–$(C_2)_7$–CH_3 and H–$(C_2)_8$–CH_3. The absolute values of the absorbance in (c) and (d) are estimated from those of diluted solutions. [46] Reprinted with permission from Elsevier

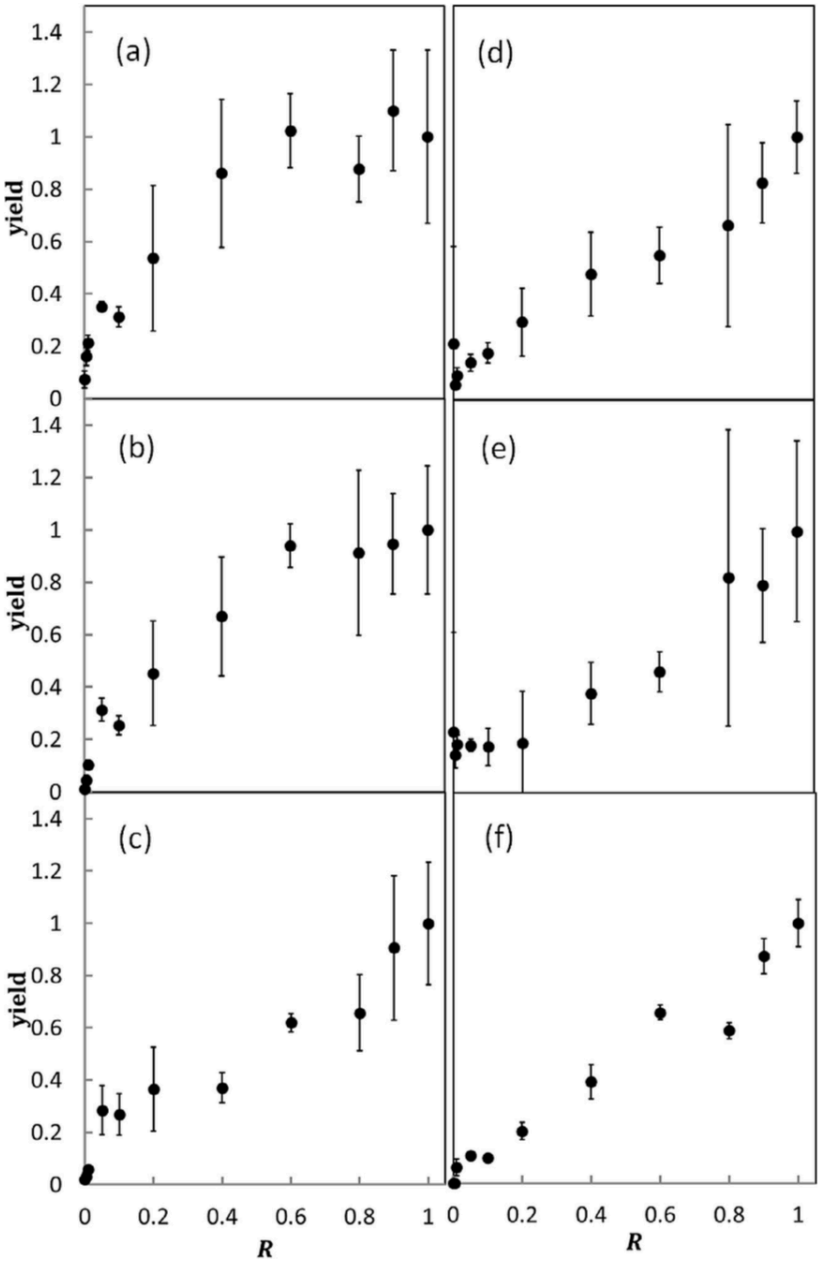

Figure 2.13. Plots of relative yield of the polyynes, (a)–(e) for C_6H_2–$C_{14}H_2$, respectively. The yields are normalized at R=1. The R-dependence of methylpolyyne (H–$(C_2)_8$–CH_3) is shown in (f). The error bars are standard deviation of four independent lots. The fluctuation of the yields is likely due to instability of the laser ablation conditions. [46] Reprinted with permission from Elsevier

Chapter 3

Materials and Methods

3.1 Analysis Techniques

In order to identify, characterize, and analyze the polyynes, UV-Vis spectroscopy, high performance liquid chromatography (HPLC), and optical emission spectroscopy are employed. The next section explains how these techniques work and are employed.

3.1.1 UV-Vis Spectroscopy

The ultraviolet-visible spectrometer uses light in the ultraviolet-visible spectral region, around 200-800 nm. It could be absorption or reflectance spectroscopy. The absorption is a measurement of the electromagnetic radiation absorbed by the atoms or molecules to excite an electron from the highest occupied molecular orbital (HOMO) to the lowest unoccupied molecular orbital (LUMO). The smaller the gap between the HOMO and LUMO the longer the wavelength absorbed by the electron. The transition of the electron can only occur with a precise amount of radiation since energy levels are quantized, and only electrons with π-bond or non bonding electrons can absorb radiation in the ultraviolet-visible region. A schematic diagram of the instrument is shown in figure

3.1. Two lamps generate ultraviolet and visible light. The beams are directed to a first mirror that sends them together to a diffraction grating to separate the light to its wavelength components. A specific wavelength range appropriate for the sample can be chosen. Using a 50/50 split mirror, the beam is then split into two beams: one goes to the sample, and the other one goes to a reference solvent. The reference can be any transparent and non-absorbing solvent such as water, methanol or hexane. In the polyynes synthesis experiments, hexane is used mostly to capture the polyynes produced, so hexane is used as a reference in the UV-Vis absorption analysis as well. The sample and the reference should be contained in glass or quartz cuvettes, and both cuvettes should be identical, and should be cleaned well prior to every reading to avoid contamination. The light that passes through is detected and the intensity of the light is measured. The absorbance (A) is then calculated according to the equation:

$$A = log_{10}\left(\frac{I_o}{I}\right)$$

Where I_o is the intensity of the light passes through the reference, and I is the intensity of the light that passes through the sample. If there is no light absorption from the target aimed to be studied, $I = I_o \Rightarrow A = 0$. The data are given as a chart of absorbance against wavelength. The UV-Vis spectrometer, and the principal analytical technique used for this study is a ParkinElmer, LAMBDA 1050 equipped with a tungsten-halogen visible lamp and a deuterium ultraviolet lamp. The instrument is located at WATLab room 080 in the chemistry 2 building in the University of Waterloo, Waterloo, Canada. Images taken of the spectrometer and its cuvettes chamber are shown in figure 3.2. The reference cuvette should be placed in the back holder and the sample in the front holder.

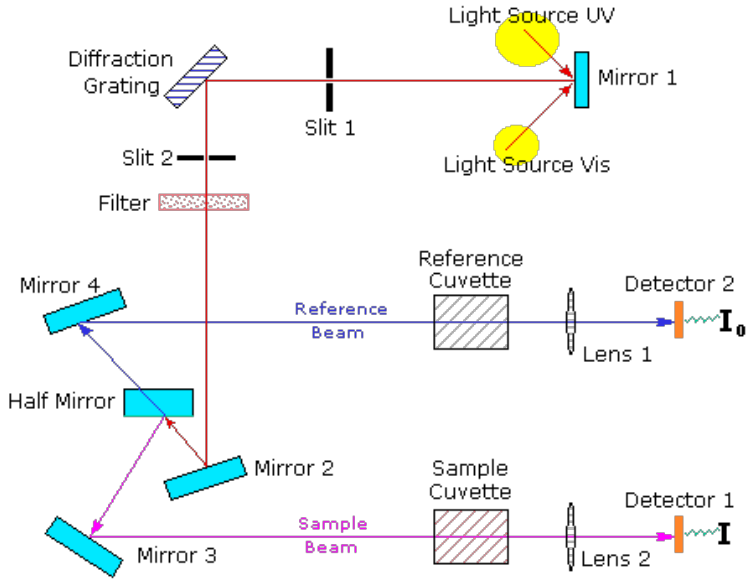

Figure 3.1. A schematic diagram of the components of a typical UV-Vis spectrometer

Figure 3.2. (a) The UV-Vis spectrometer located at WATLab room 080 in the chemistry 2 building. (b) The holders chamber for the sample and reference cuvettes.

3.1.2 High Performance Liquid Chromatography (HPLC)

In the case of highly concentrated solutions or solvents that have absorption peaks around the position of polyynes' peaks, standard UV-Vis spectroscopy cannot be employed. The polyynes in the solution will need to be purified and separated form the solution and from each other, and then identified. An instrument that can do both and also quantify the product is the HPLC. Using a pump that produces high pressure, the small amount of the solution injected in the device is passed to a column filled with a solid adsorbent material (e.g. silica) that mixture components interact differently with making them flow with different rates, thus separated and characterized individually. Due to the unavailability of the proper HPLC setup specialized for polyynes in the University of waterloo, samples need to be analyzed with HPLC were shipped to our collaborators, Prof. Wakabayashi Tomonari and his group based in Kindai University, Department of Chemistry, in Osaka, Japan. The instrument is a Shimadzu LC-10A liquid chromatographic system equipped with a Wakosil 5C18AR polymeric octadecyl silica (ODS) Column in a reversed phase, and coupled with UV-Vis detector. Only 0.1 mL of the sample is injected in the HPLC, and it runs for 10 minutes retention time. A UV-Vis absorption reading is taken every second resulting in 600 spectra for every sample. The data all together can be plotted in a 3D chromatographs that show all the polyynes and at what retention time they were detected.

3.1.3 Optical Emission Spectroscopy

During the LIB experiments a formation of plasma around the focus point and a visible photon emission was observed (see figure 3.3 (a)). This was characterized using a fiber spectrometer (Ocean Optics USB4000) (figue 3.3 (b)). The emission spectra confirms whether C2 is formed or not by looking for the swan bands in the spectrum, which helps in understanding the formation mechanism of polyynes. Swan bands are a sequence of peaks in the visible spectral region characteristic of the presence of C2.

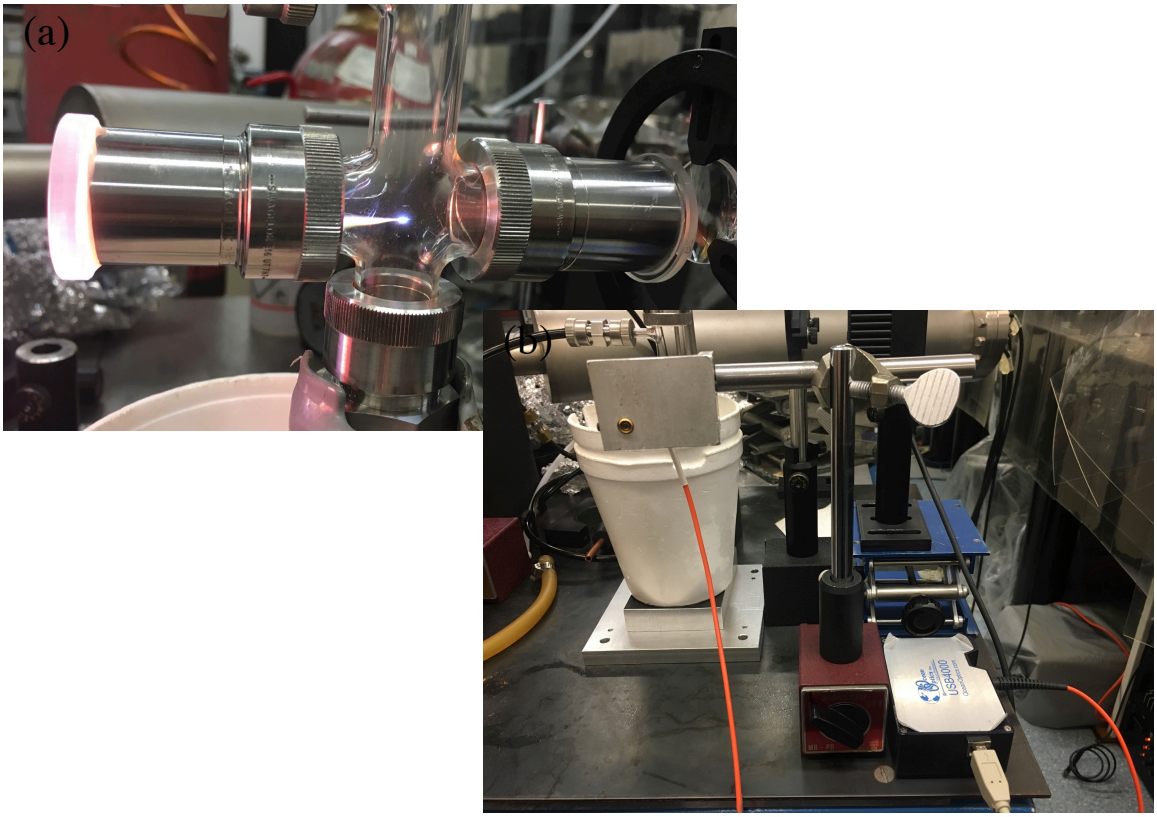

Figure 3.3. (a) An image taken during the fs LIB in gaseous hydocarbons shows the plasma formation and the visible photon emission. (b) The optical emission spectrometer used for characterization of the formed plasma and photon emission.

3.2 Polyyne Synthesis Experiments

Laser interaction with the matter in its liquid, gaseous and solid state has been used to form polyynes in this work. This section will include a description of the setups and procedures of these experiments, The results obtained, and a discussion of the results will be illustrated in the following section.

3.2.1 Liquid Irradiation

Laser irradiation of organic liquids was investigated first following a work done in our lab previously [37]. A schematic drawing and an image of the experiment setup are shown in figure 3.5. A small amount of the liquid, around 2 mL, in a small vial is irradiated with fs laser. The fs laser is an amplified Ti:Sapphire laser with 800 nm wavelength and 1 KHz repetition rate, generates pulses with 35 fs duration. This laser is located at the physics department room 119 at the University of waterloo in Waterloo, Canada. Using a 5 cm focusing lens, the laser is focused at the meniscus of the solvent forming a vapor on top of the liquid surface and a filament along the vapor and the inside of the solvent. In the previous work, toluene was the target, and a formation of H-capped polyynes and methylpolyynes were reported [37]. Toluene consists of a benzene ring attached to one methyl group, so xylene was chosen as a target for this work to study the influence of methyl group existence in the target molecules on the formation of methylpolyynes since xylene has two methyl groups attached to the benzene ring instead of one. Xylene isomers (o-xylene, m-xylene, and p-xylene) were irradiated with the fs

laser at energies around 0.3 and 0.5 mJ/pulse for 3 and 4 hours. During the irradiation, samples turned gradually to brownish yellow and black insoluble carbon particles formed on the surface as shown in figure 3.6, where an image was taking every half an hour during the irradiation. The standard UV-Vis spectrometer cannot be employed directly on the samples since xylene has identifying peaks around the polyyne peak positions, which could mask them. Therefore, the samples were filtered after the irradiation with a syringe filter with 0.2 μm pore size, and then HPLC was employed to purify the polyynes first and then characterize them with a coupled UV-Vis spectrometer.

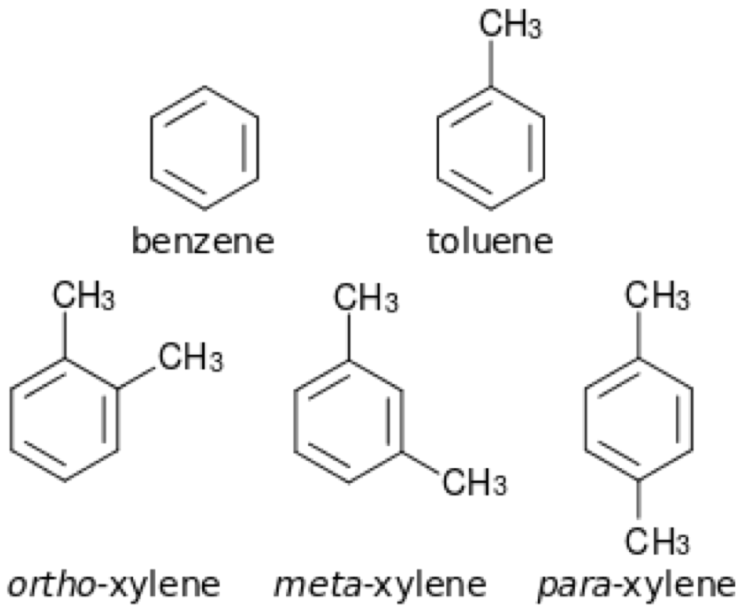

Figure 3.4. Molecular structure of benzene (C6H6), toluene (C7H8), and xylene isomers (C8H10).

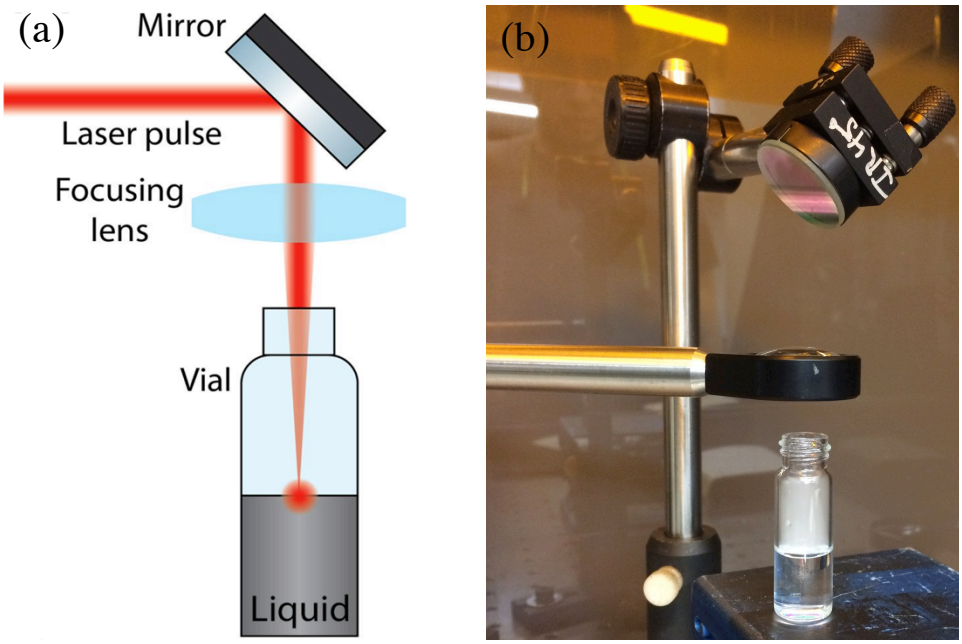

Figure 3.5. (a) a schematic drawing of the fs laser irradiation of xylene. [37] Reprinted with permission from Elsevier (b) an image taken of the setup in real life.

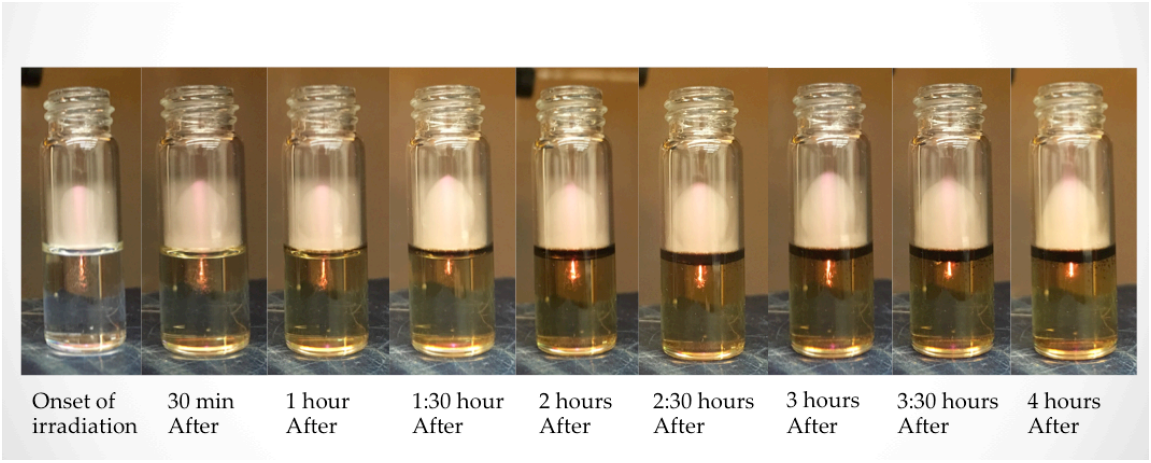

Figure 3.6. Images taken every 30min of m-xylene sample irradiated with fs laser at 0.5 mJ/pulse for 4 hours.

3.2.2 Laser Induced Breakdown (LIB)

A LIB experiment is onewhich involves laser irradiation of the matter in it's gas phase, where the number of hydrocarbon molecules are less and more controllable than in a liquid. A schematic drawing of the experiment setup is show in figure 3.9. Argon gas with high purity 99.9999% is sent to the container where the organic solvent is kept. A flow meter is placed between the argon gas and the organic solvent to control the flow rate of the argon and to keep it fixed. The argon bubbles inside the solvent carry the hydrocarbon molecules to the irradiation cell. The left and right sides of the irradiation cell are closed with glass windows to allow the laser to go through. The bottom of the irradiation cell where the gas exits the cell, is cone-shaped to another cell that contains 5 mL of cooled hexane liquid prepared for the capture of the product of the irradiation. The hexane is cooled using a coolant kept at -80℃. In the setup used, the coolant is methanol cooled down using liquid nitrogen to keep the irradiation cell contamination-free. Hexane (C6H14) with high purity 99.99% is chosen as the target molecule for this setup.

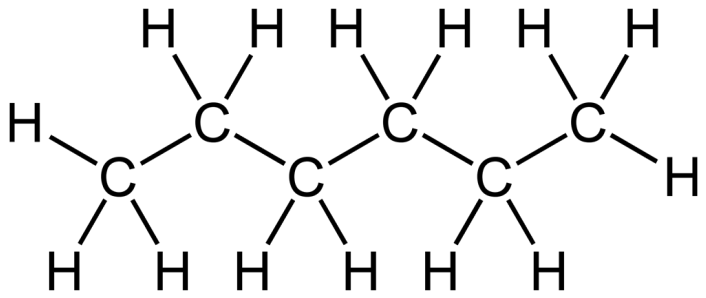

Figure 3.7. Molecular structure of normal hexane C6H14

The laser is focused using a lens with 70 mm with the ns laser and 80 mm with the fs laser focal length in the center of the irradiation cell leading to a plasma formation. The fs laser used here is the same fs laser used in the liquid irradiation experiment. A LIB experiment in hexane was also done with a ns laser. The ns laser used is located in the chemistry department at Tokyo Metropolitan University (TMU) in Tokyo, Japan. It is an Nd:YAG laser (Spectra Physics Pro-290), with 30 Hz repetition rate and 532 nm wavelength. The laser generates an average energy of 150 mJ/pulse. Two hexane samples were irradiated with the fs laser with 1.6 mJ/pulse and 2 mJ/pulse, for 60 Sec and 50 mL/min argon flow rate, whereas with the ns laser the output energy was kept fixed at 150 mJ/pulse and two hexane samples were irradiated at different flow rates, 50mL/min and 100mL/min, for 60 Sec. After the irradiation, samples were filtered with a syringe filter with 0.2 μm pore size. The emission from plasma formed during the fs LIB was characterized using the fiber spectrometer.

The LIB can also be done directly in gaseous hydrocarbons either by mixing them with argon or without the aid of argon as shown in figure 3.10. In this work, ethylene gas (C2H4) was irradiated with fs laser at 4 different pulse energies (0.6, 1, 1.5, 2 mJ/pulse), and later on two samples were irradiated with the ns laser, but at different flow rates (50, 100 mL/min), all for 60 Sec. Also with the ns laser, LIB was done in propane gas (C3H8) at 25 and 50 mL/min flow rates for 60 Sec, and in acetylene (C2H2), but the irradiation time dependency was focused on by irradiating for 20, 30, 40, 50, and 60 Sec, and the flow rate was fixed at 50 mL/min. The emission spectrum of the plasma formed with the fs LIB in ethylene was taken. All the samples were filtered prior to the UV-Vis spectrometer employment. In the case of acetylene, hexane is cooled using a coolant kept at -40℃ instead of -80℃.

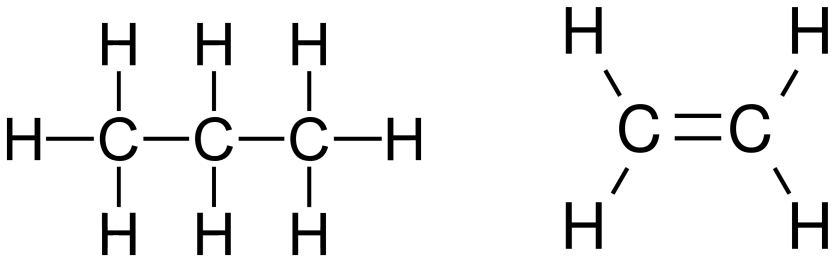

Propane Ethylene

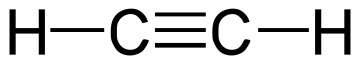

Acetylene

Figure 3.8. Molecular structure of propane C3H8, ethylene C2H4, and acetylene C2H2

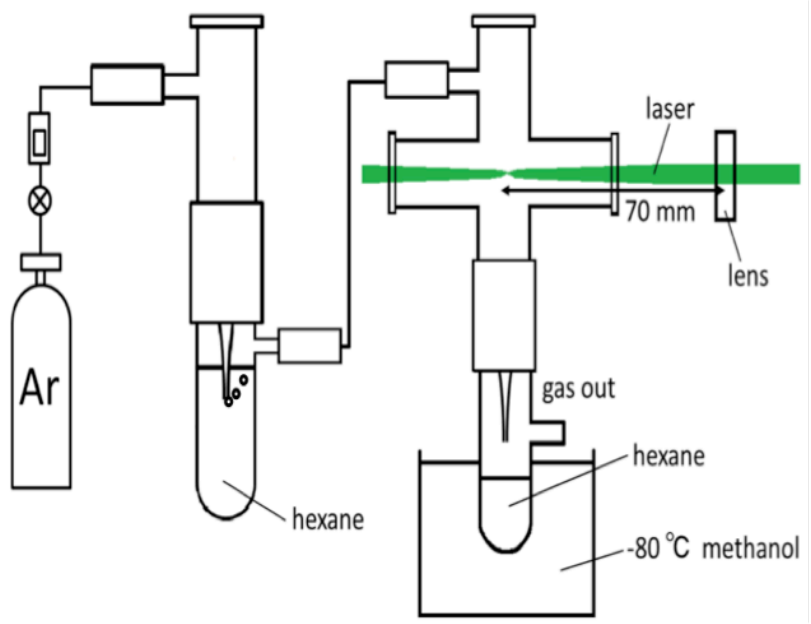

Figure 3.9. Schematic drawing of the LIB by bubbling argon in hexane experimental setup. The laser is either ns or fs laser. [53] Reprinted with permission from Elsevier

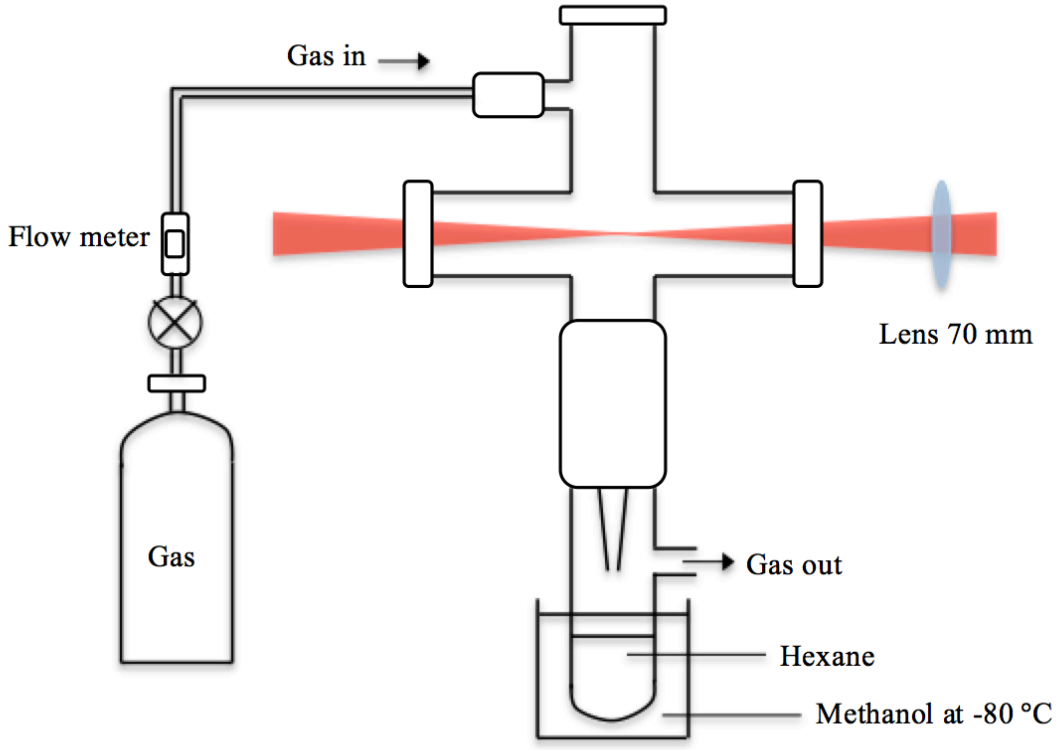

Figure 3.10. Schematic drawing of the LIB directly in hydrocarbon gases experimental setup. The laser is either ns or fs laser, and the gas cylinder is either propane, ethylene or acetylene.

3.2.3 Laser Ablation of Graphite

In a similar experiment to LIB and with a similar setup except for the irradiation cell, the setup is shown in figure 3.11, graphite is ablated with ns laser in the existence of hydrocarbon gas flow. A disc of graphite that has many small pores with diameters of 1 mm in it to allow the gas to go through is placed inside the irradiation cell making a 45° angle with the direction of the laser beam line. A focusing lens with 40cm focal length was placed 20 cm away from the graphite disc making a 30 mm^2 interaction surface area between the laser and the disc. The ns laser used for the laser ablation is different from the one used for the ns LIB. It is an Nd:YAG laser with 10 Hz repetition rate and 532 nm wavelength. The laser generates an average energy of 150 mJ/pulse, and also located in the chemistry department at Tokyo Metropolitan University (TMU) in Tokyo, Japan. Firstly, graphite was ablated in argon/propane mixture gas flow. Two samples were obtained: the first one at a propane ratio R = 0.5 where R = $f_p/(f_p + f_a)$, and f_p and f_a are the propane and the argon flow rates respectively, the second samples was at a propane ratio R = 0.75. Secondly, one sample was obtained from laser ablation of graphite in acetylene gas flow (R = 1). Both experiments were done for 1 min duration. Samples were filtered with a syringe filter with 0.2 μm pore size after the laser ablation, and then UV-Vis spectroscopy was employed.

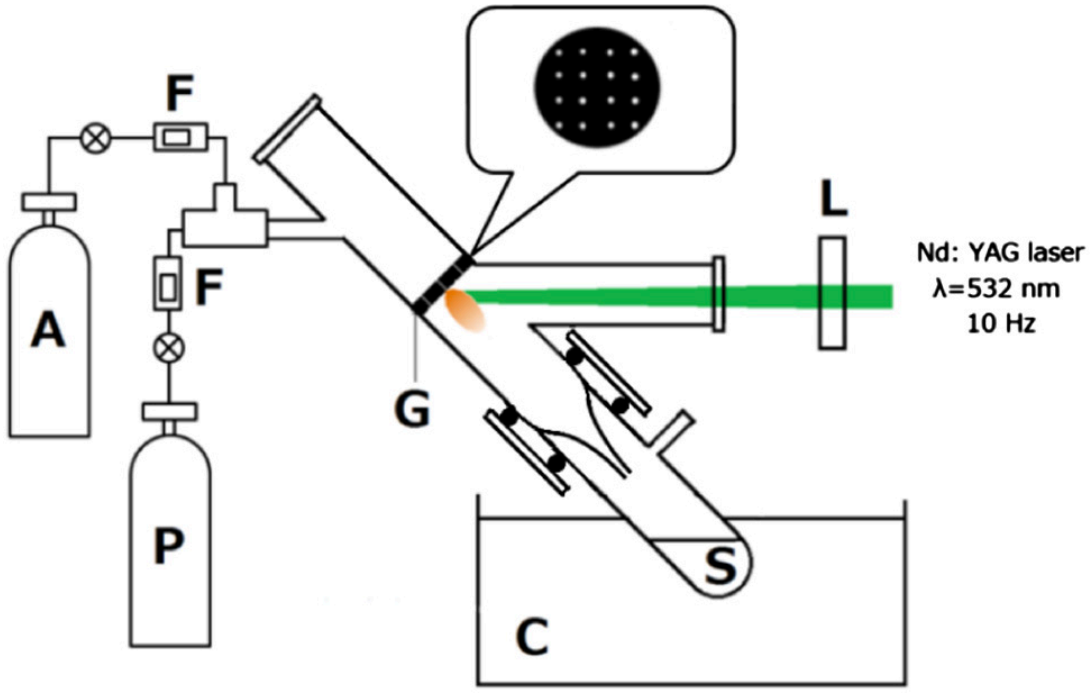

Figure 3.11. Schematic drawing of the experimental setup designed for efficient capture of the laser ablation products. A: pure Ar gas cylinder, P: propane or Ar/propane gas cylinder, F: flow meter, S: organic solvent, C: coolant, G: Graphite target, L: lens. The inset shows the top view of the target. [46] Reprinted with permission from Elsevier

3.3 Results and Discussion

Because of the formation of large insoluble carbon particles even if not seen by the naked eye, all the resulted samples were filtered with an HPLC-ideal chromatography syringe filter with 2 μm pores, and then sent for analysis. Xylene samples were shipped to our collaborators in Kindai University for HPLC analysis. The plotted 3D HPLC chromatograms of the irradiated o-xylene, m-xylene, and p-xylene are shown in the figures 3.12, 3.13, and 3.14. The samples were analyzed in the order shown in the images. This is important since the 10 minutes, running time of the HPLC, was not enough to detect the longer polyynes, and the polyynes C14H2 and C16H2 are detected in the next analyzed sample irradiated and shown in its chromatogram. From these chromatograms, the retention time at which each polyyne is detected is noted, and then the absorption readings that were taking at the same seconds were plotted. Figure 3.15 is a view of the plotted absorption spectra of the pure polyynes obtained by the m-xylene irradiation at 0.5 mJ/pulse for 4 hours all together (a) and separately (b). Figure 3.16 is the absorption spectra of the pure C10H2 and C12H2 resulted from the irradiation of o-Xylene (a) and (b) for 3 hours and (c) and (d) for 4 hours. The absorption spectra of the products resulted from the LIB by bubbling argon in organic liquids or directly in hydrocarbon gases and from laser ablation of graphite are shown in figures 3.17, 3.18, 3.19, 3.21, 3.24, and 3.25. The emission spectra obtained from LIB in hexane and ethylene are plotted in figure 3.23. The 3D chromatograms, the absorption spectra of the LIB and laser ablation of graphite, and the emission spectra were plotted using Igor pro, a scientific data analysis software.

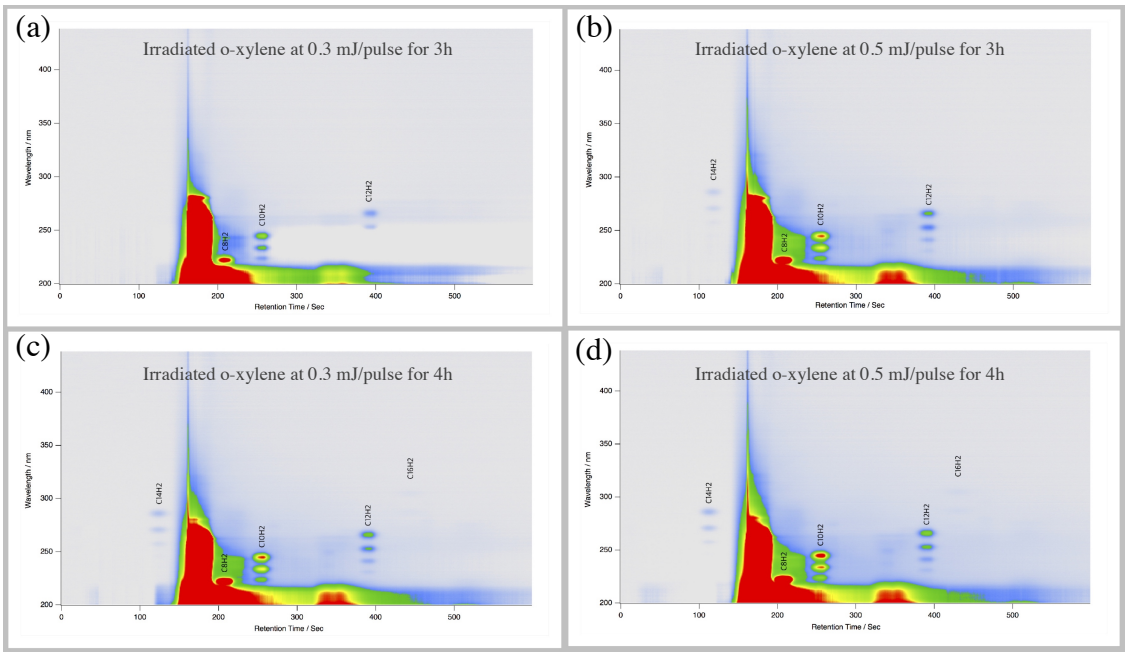

Figure 3.12. HPLC chromatograms of the fs laser irradiated o-xylene at: (a) 0.3 mJ/pulse, for 3h. (b) 0.5 mJ/pulse, for 3h. (c) 0.3 mJ/pulse, for 4h. (d) 0.5 mJ/pulse, for 4h.

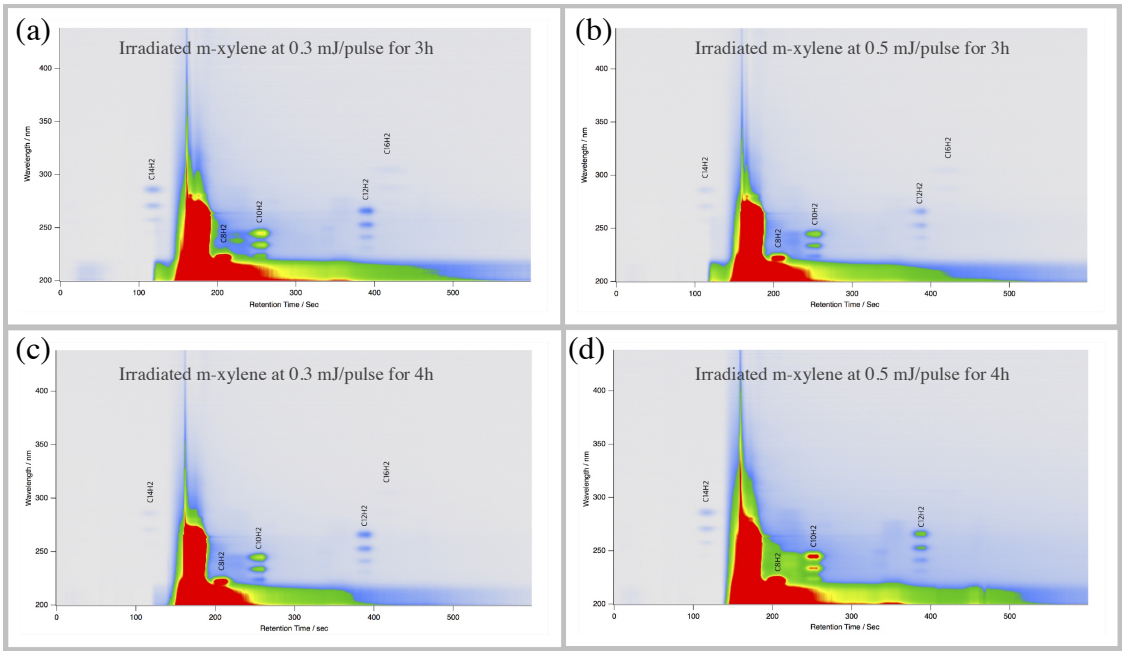

Figure 3.13.HPLC chromatograms of the fs laser irradiated m-xylene at: (a) 0.3 mJ/pulse, for 3h. (b) 0.5 mJ/pulse, for 3h. (c) 0.3 mJ/pulse, for 4h. (d) 0.5 mJ/pulse, for 4h.

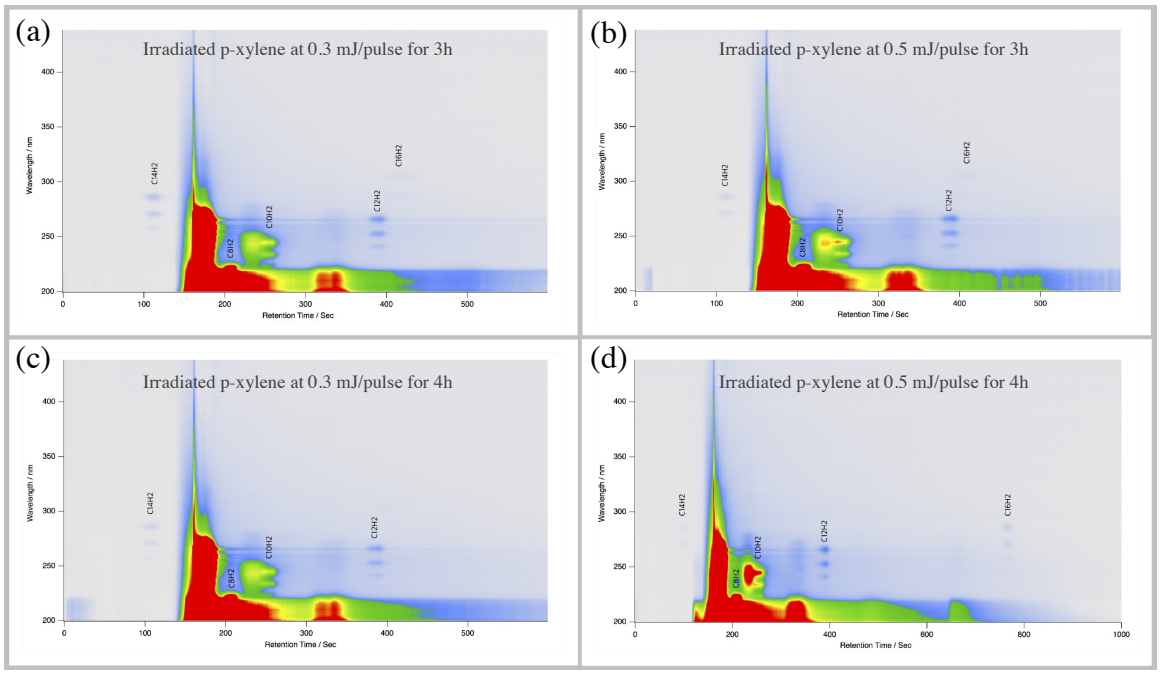

Figure 3.14. HPLC chromatograms of the fs laser irradiated p-xylene at: (a) 0.3 mJ/pulse, for 3h. (b) 0.5 mJ/pulse, for 3h. (c) 0.3 mJ/pulse, for 4h. (d) 0.5 mJ/pulse, for 4h.

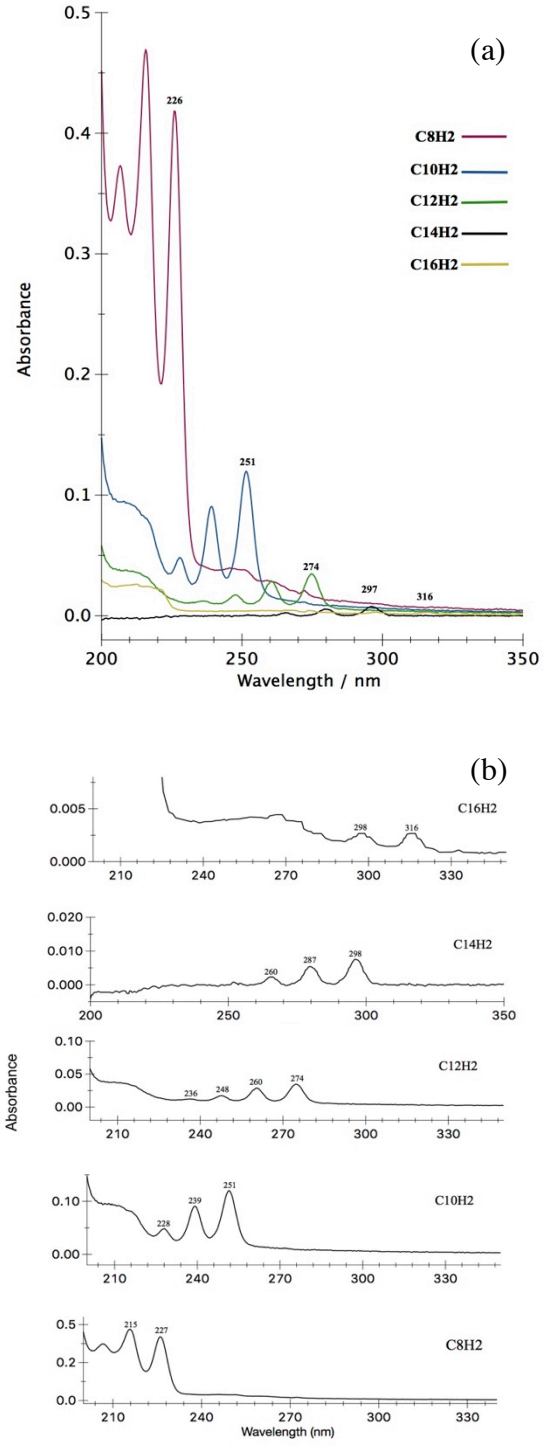

Figure 3.15. UV-Vis absorption spectra of the pure polyynes resulted from the fs laser irradiation of m-Xylene at 0.5 mJ/pulse for 4 h. (a) Sharing the axes. (b) Separated.

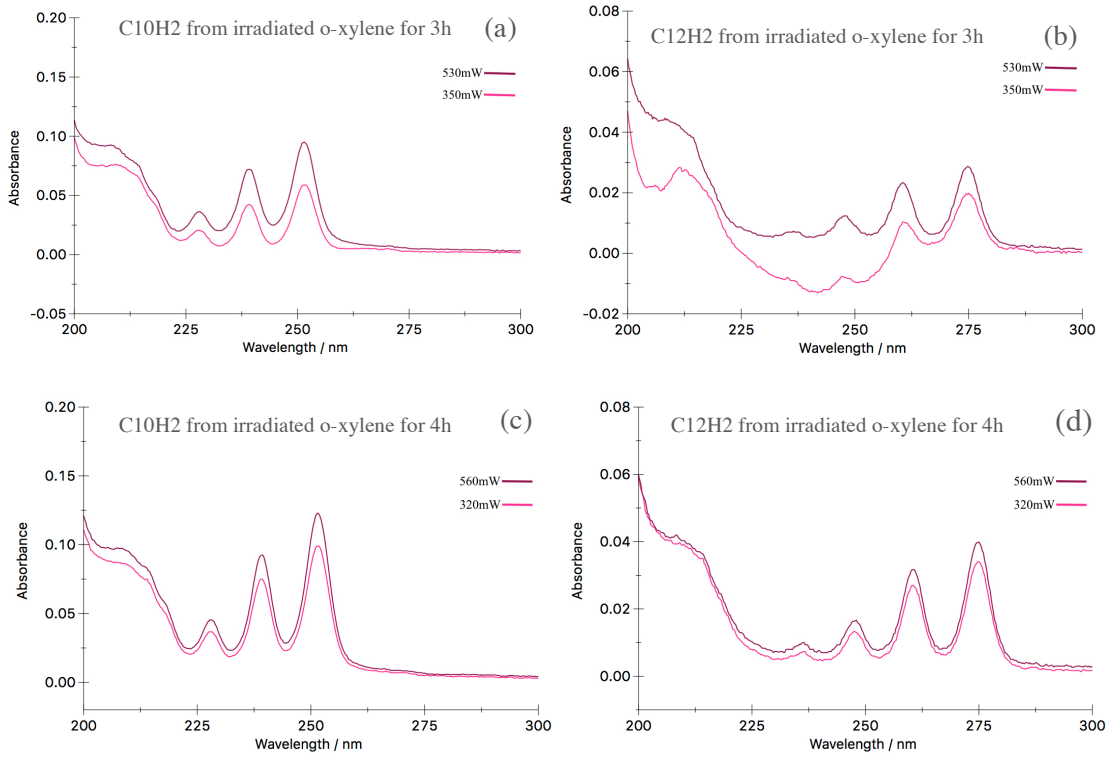

Figure 3.16 UV-Vis absorption spectra of the pure polyynes (C10H2 and C12H2) resulted from the fs laser irradiation of o-Xylene (a) and (b) for 3 hours and (c) and (d) for 4 hours.

As can be seen in the HPLC chromatograms shown in the figures 3.12, 3.13 and 3.14 of the irradiated xylene isomers, and in the absorption spectra of the purified polyynes resulted from the fs laser irradiation of m-Xylene at 0.5 mJ/pulse for 4h shown in figure 3.15, H-capped polyynes from C8H2 to C16H2 were observed in the samples resulted from the fs laser irradiation of xylene isomers. Individual polyynes were identified by their distinct peaks that correspond to the previously reported peak positions by [44] and [49]. No significant influence of the type of the isomer on the results was noticed, only small differences that could be due to the experiment conditions that are hard to control and to keep exactly the same with every sample. It was suggested by [37] after the fs laser irradiation of toluene, the experiment that was carried out previously in our lab, that the end cap of the polyynes produced could be controlled by choosing a specific target since choosing toluene resulted in the production of methylpolyynes, polyynes capped with methyl group instead of hydrogen at one end. The formation of methylpolyynes from the fs laser irradiation of xylene with the same rate, with higher rate or with methyl group at each end was expected since xylene has two methyl groups attached to the benzene ring. However, no formation of methylpolyynes was observed from the fs laser irradiation of xylene. This could be because of the existence of two methyl groups instead of one and they interact with each other when the xylene molecule is broken. The plotted absorption spectra of the purified C10H2 and C12H2 in figure 3.16 show that the absorbance, representing the amount of polyynes produced, increases with higher energy and longer irradiation time witch is expected since more energy and longer irradiation time are expected to break more molecules and produce more polyynes.

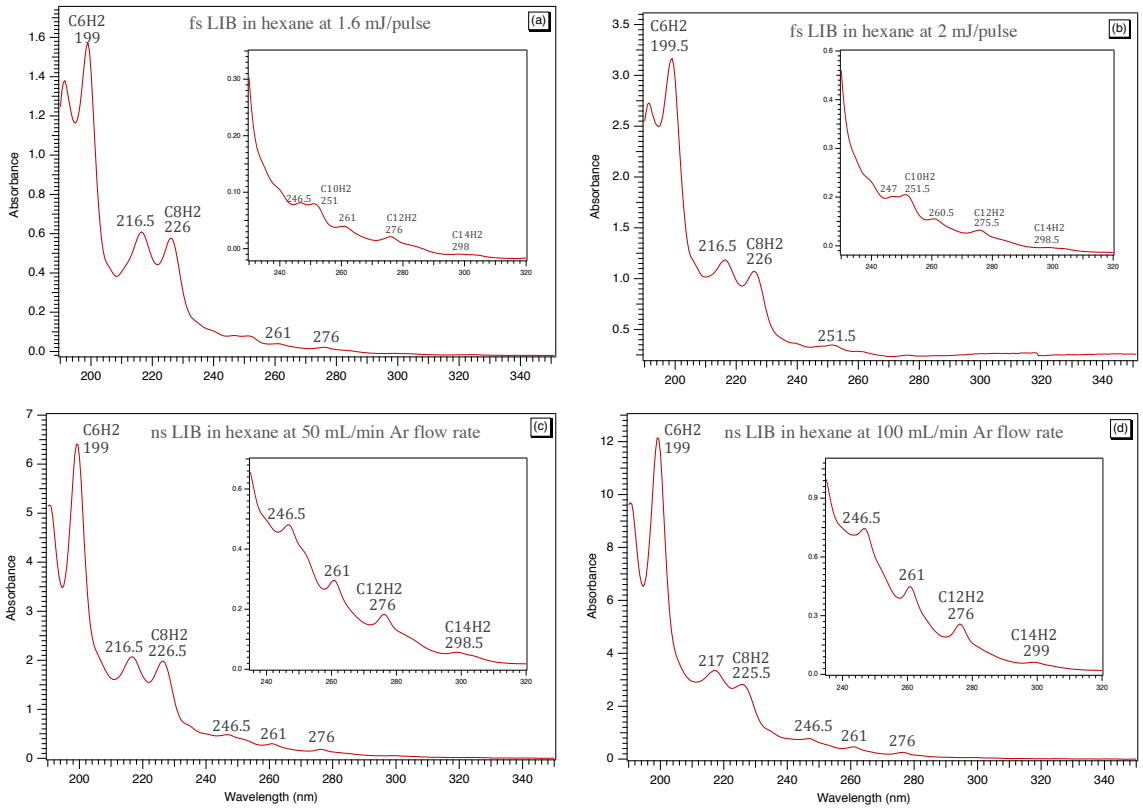

Figure 3.17. UV-Vis absorption spectra of the products resulted from: (a) fs LIB in hexane at 1.6 mJ/pulse. (b) fs LIB in hexane at 2 mJ/pulse. (c) ns LIB in hexane at 50 mL/min Ar flow rate. (d) ns LIB in hexane at 100 mL/min Ar flow rate. An expanded scale is shown in the indexes for a better view of longer polyynes.

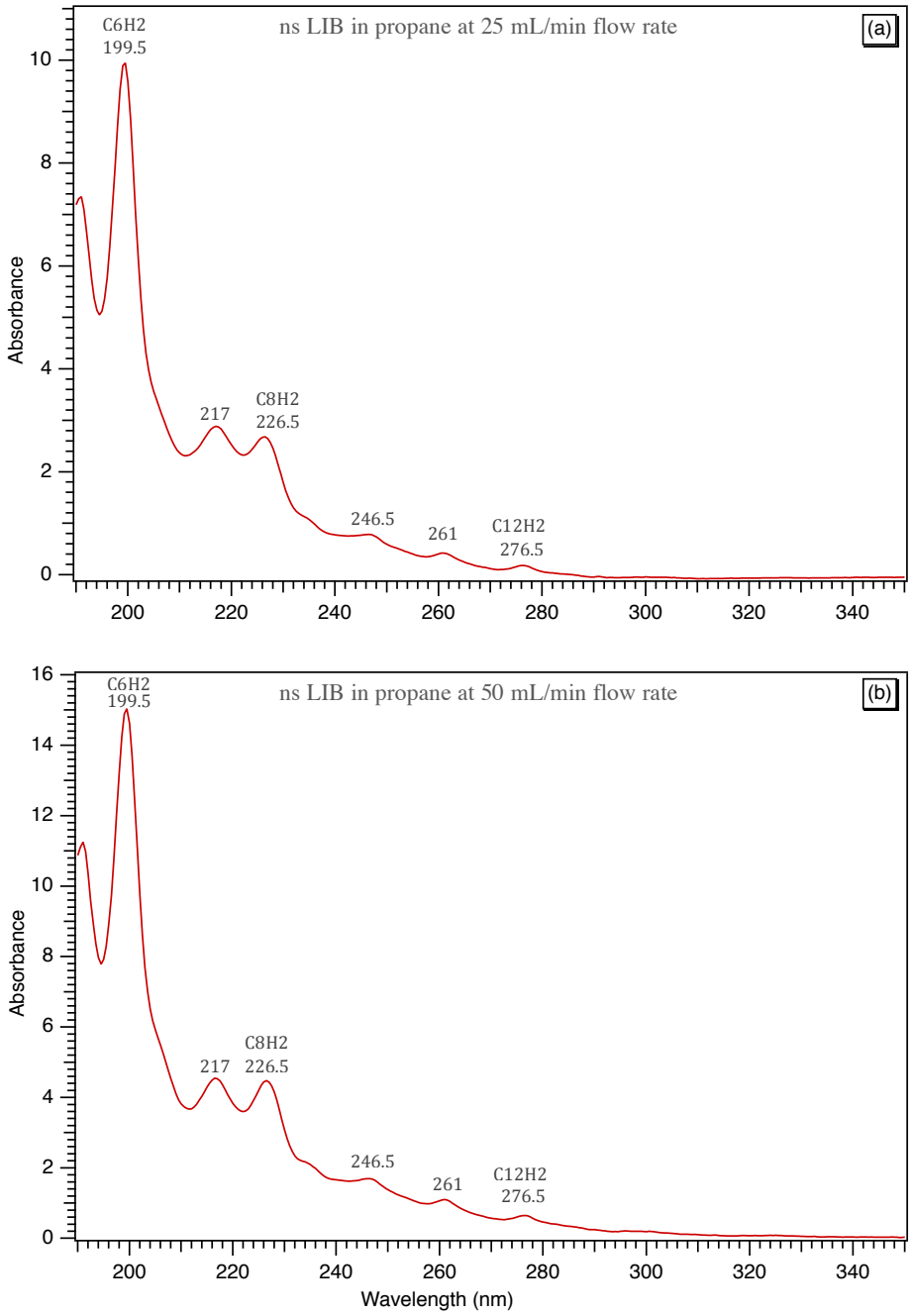

Figure 3.18. UV-Vis absorption spectra of the products resulted from: (a) ns LIB in propane at 25 mL/min flow rate. (b) ns LIB in propane at 50 mL/min flow rate.

The fs LIB in hexane results are shown in figure 3.17 (a) and 3.17 (b). The formation of polyynes from C6H2 to C14H2, and with higher absorbance when higher energy is used is observed. The polyynes peaks and the positions they appear at are indicated in the graphs. The peak positions agree with those reported by [44] and [49] (review table 2.1). In contrast, the ns LIB in hexane, can be shown in figure 3.17 (c) and 3.17 (d), resulted in the formation of the polyynes C6H2, C8H2, C12H2, and C14H2. The peak of C10H2 should appear at around 251nm wavelength, but it cannot be seen. It's assumed that the C10H2 peak overlapped with the polyyne C12H2 peak that appears at 246.5nm. The concentration of polyynes resulting from the ns LIB in hexane is significantly higher than that resulting from fs LIB in hexane. When the argon flow bubbled in the hexane was increased to 100 mL/min, the amount of polyynes formed were doubled. Absorption spectra obtained from the ns LIB in propane are plotted in figure 3.18. Although C6H2 – C12H2 polyynes were formed from the ns LIB directly in propane but not C14H2, the ns LIB in propane at 50 mL/min propane flow rate resulted in 2.3 times the amount of polyynes from ns LIB in hexane at the 50 mL/min argon flow rate. Therefore, the LIB experiment is more efficient when carried out directly in gaseous hydrocarbon molecules instead of bubbling argon in liquid hydrocarbon molecules to form a vapor. However, there's a tendency to a peak around 300 nm where the peak of C14H2 should appear in the spectrum in figure 3.18 (b). This could mean that C14H2 was formed but in a very limited amount.

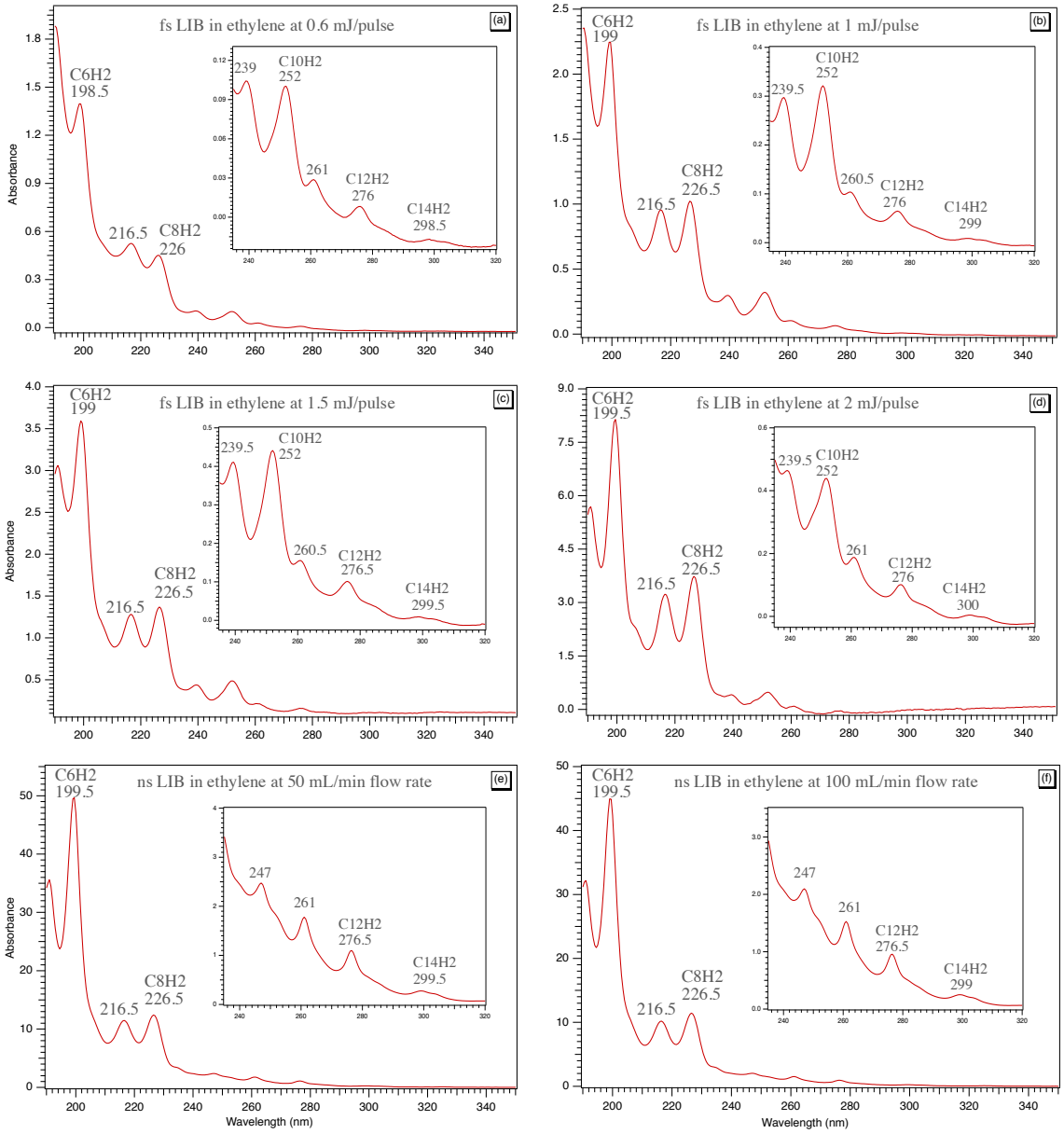

Figure 3.19. UV-Vis absorption spectra of the products resulted from: (a) fs LIB in ethylene at 0.6 mJ/pulse. (b) fs LIB in ethylene at 1 mJ/pulse. (c) fs LIB in ethylene at 1.5 mJ/pulse. (d) fs LIB in ethylene at 2 mJ/pulse. (e) ns LIB in ethylene at 50 mL/min flow rate. (f) ns LIB in hexane at 100 mL/min flow rate. An expanded scale is shown in the indexes for a better view of longer polyynes.

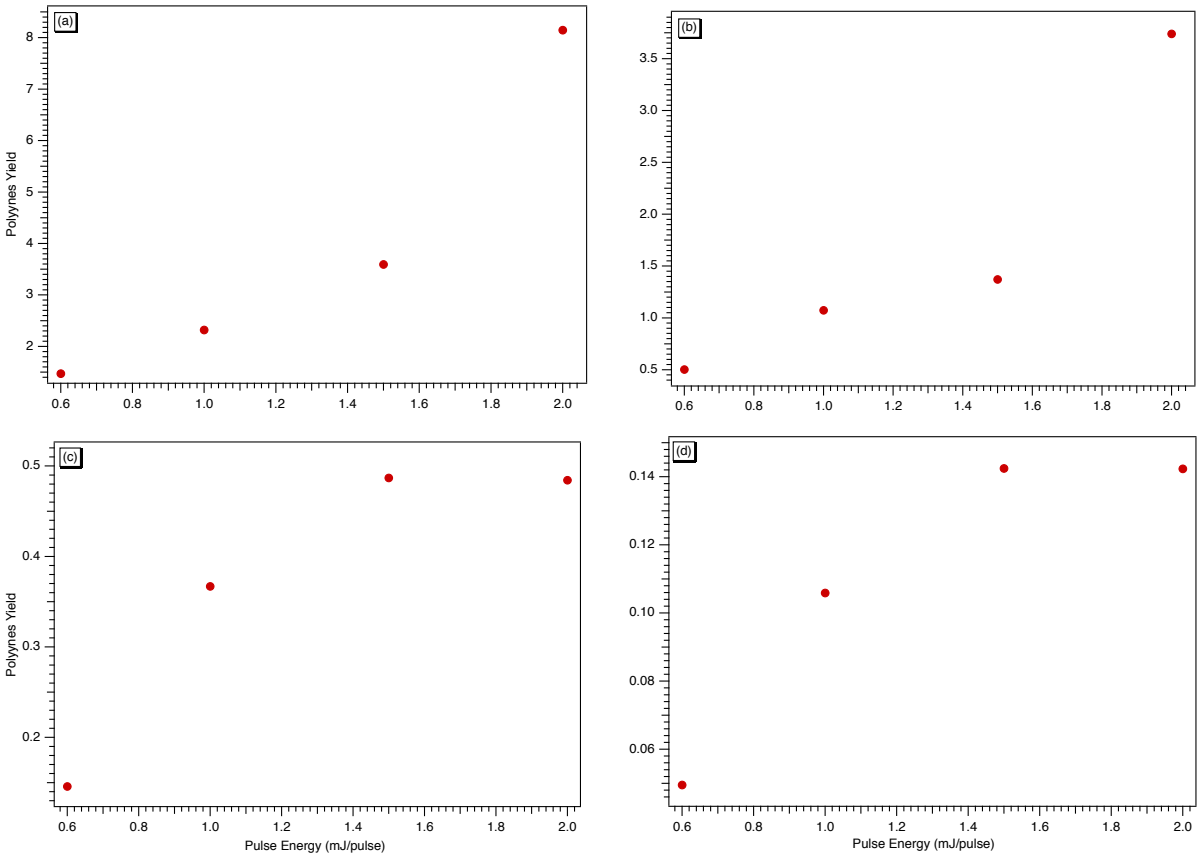

Figure 3.20. The estimated polyyne yield of the products resulted from fs LIB in ethylene as a function of pulse energy: (a) C6H2. (b) C8H2. (c) C10H2. (d) C12H2.

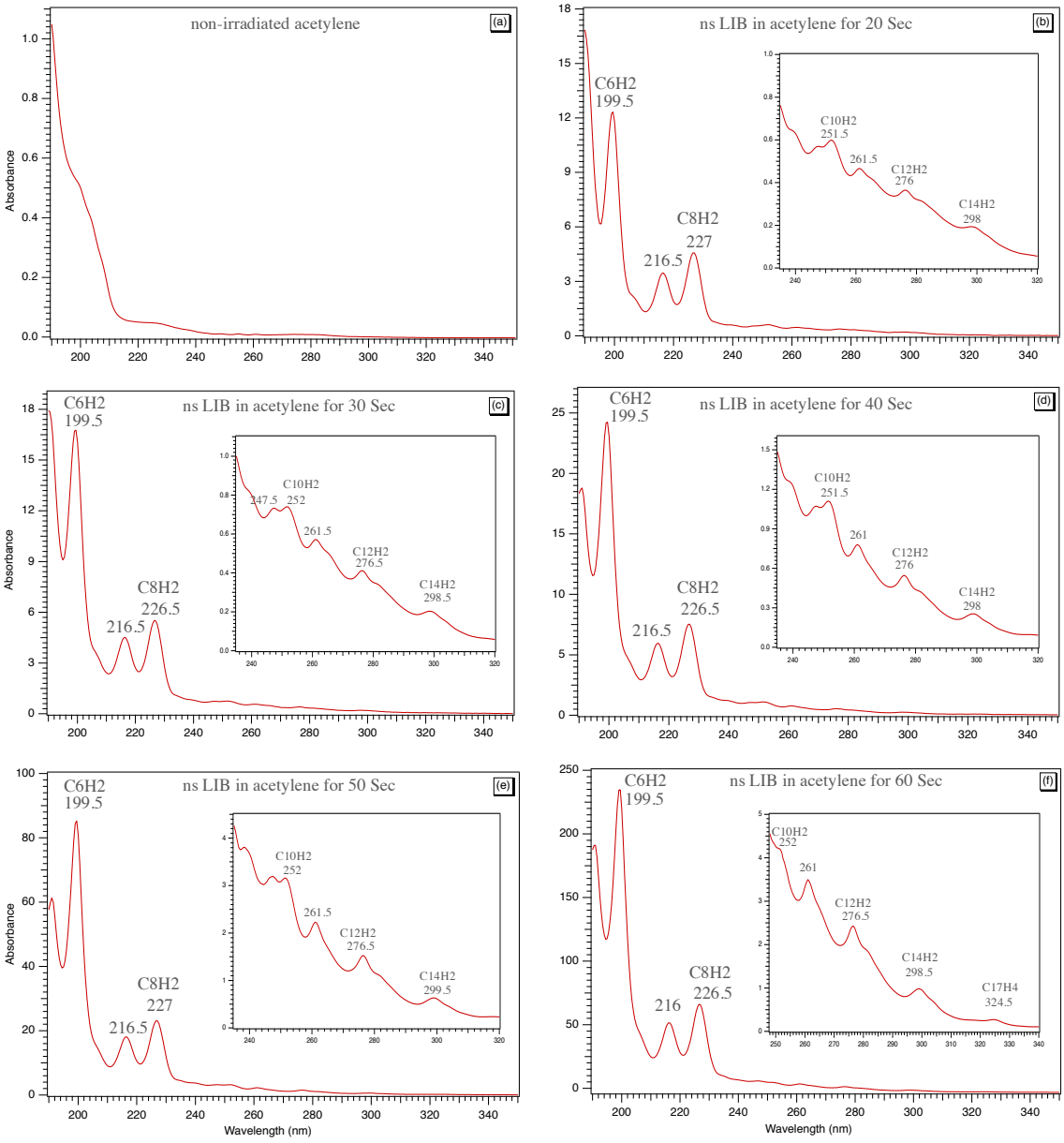

Figure 3.21. (a) UV-Vis absorption spectrum of non-irradiated acetylene. UV-Vis absorption spectra of the products resulted from: (b) ns LIB in acetylene for 20 Sec. (c) ns LIB in acetylene for 30 Sec. (d) ns LIB in acetylene for 40 Sec. (e) ns LIB in acetylene for 50 Sec. (f) ns LIB in acetylene for 60 Sec. An expanded scale is shown in the indexes for a better view of longer polyynes.

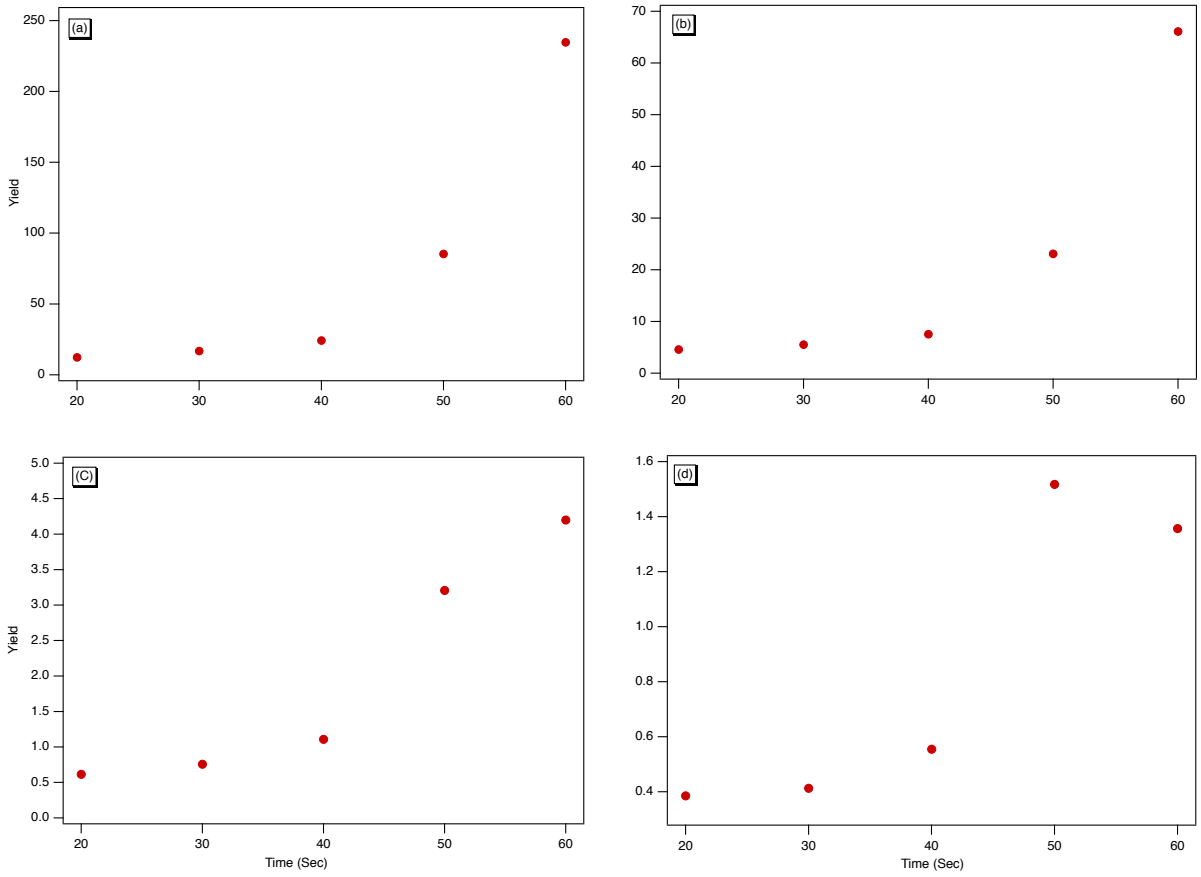

Figure 3.22. The estimated polyyne yield of the products resulted from ns LIB in acetylene as a function of time: (a) C6H2. (b) C8H2. (c) C10H2. (d) C12H2.

Further LIB studies directly in hydrocarbon gases were carried out in ethylene and acetylene focused on investigating the laser energy and the irradiation time dependency in the formation of polyynes. In the case of ethylene (see figure 3.19) C6H2 – C14H2 were produced from both ns LIB and fs LIB with a significant difference in the polyyne yield. Polyynes produced by ns LIB in ethylene at 50 mL/min flow rate and 150 mJ/pulse energy are 6 times those produced by fs LIB in ethylene at the same flow rate and 2 mJ/ pulse energy. Similarly, the absorbance of polyynes increases with the increasing energy and gas flow rate. Figure 3.20 shows the estimated polyyne yield of the products resulting from fs LIB in ethylene as a function of pulse energy. As can be seen, C6h2 increases exponentially with the energy increase, C8H2 increases as well with the increasing energy, C10H2 and C12H2 increases until 1.5 mJ/pulse energy and then saturate. In the case of ns LIB in acetylene (see figure 3.21), H-capped polyynes from C6H2 to C14H2 and also the methylPolyyne H-C16-CH3 are synthesized. The peak of C17H4 was observed at 325 nm. The highest yield of polyynes reported in this work is this one obtained by the ns LIB in acetylene. The irradiation time was the focus here. The estimated polyyne yield of the products resulting from ns LIB in acetylene as a function of time is plotted in figure 3.22. As can be seen, an exponential increase in the C6H2 and C8H2 as a function of the irradiation time is clearly noticed. However, C10H2 increases exponentially until 50 seconds and then a lower increase occurs, and C12H2 increases exponentially until 50 seconds and then a decrease is observed. A hypothesis suggested here of why polyyne yield saturate or decrease for longer polyynes at higher pulse energy and at longer irradiation time is that since the longer the polyynes the less stable they are, when more longer polyynes are produced, they might more easily cross link and interact with each others and break down to shorter polyynes.

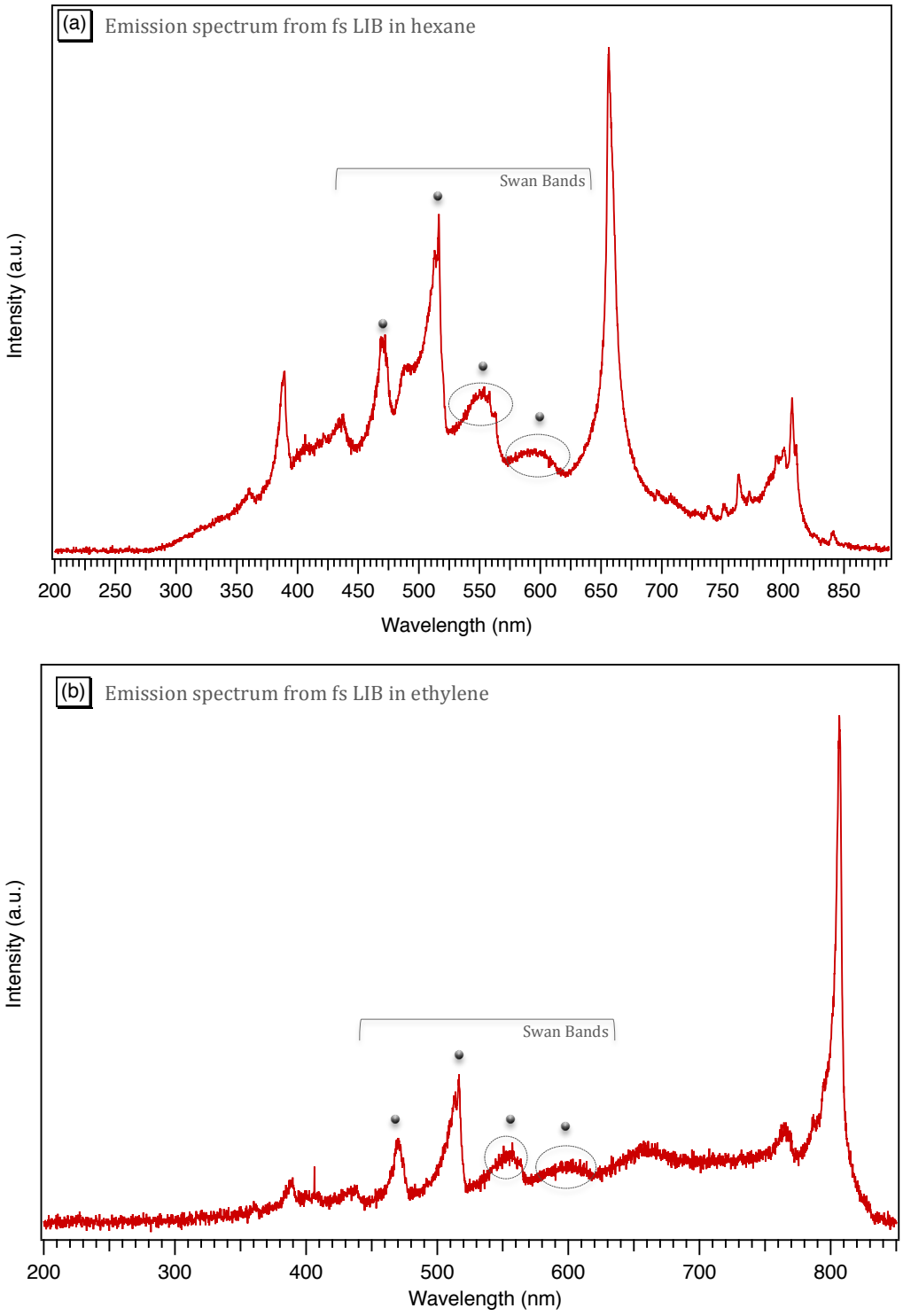

Figure 3.23. Emission spectra obtained from (a) fs LIB in hexane. (b) fs LIB in ethylene.

The swan bands are clearly seen in the emission spectra obtained from LIB in hexane and ethylene, see figure 3.23, indicating the existence of the radical diatomic carbon C2, which is an indication of a sufficient formation of carbon clusters to form polyynes. This confirm the polyyne formation mechanism of ethynyl radicals (C2H) interaction with unsaturated hydrocarbons [50, 51], and the polyyne production reaction ($C_2H + CH_3C{\equiv}CH \rightarrow C_4H_2 + CH_3$) reported by [52].

The absorption spectra obtained from the ns laser ablation of graphite experiment, which was briefly studied, in argon/propane gas mixture flow can be seen in figure 3.24. First, when the propane ratio in the argon/propane gas mixture was R = 0.5, almost no polyyne formation was observed, but when this ratio was increased to R = 0.75, polyynes from C6H2 to C14H2 was synthesized in small amounts. The ns laser ablation of graphite experiment was also carried out but in acetylene gas flow. The adsorption spectrum of the resulting sample is shown in figure 3.25. As can be seen, additional to the formation of the polyynes C6H2 to C14H2, the methylpolyyne C17H4 was also synthesized. All produced in much higher concentration. This significant increase in the polyyne production when acetylene is used indicates that the polyynes are formed not only from the graphite surface but also from the gas following in the cell. The great amount of polyynes produced when acetylene is used in the polyyne synthesis experiments might be due to its simple molecular structure that is very similar to polyyne molecular structure.

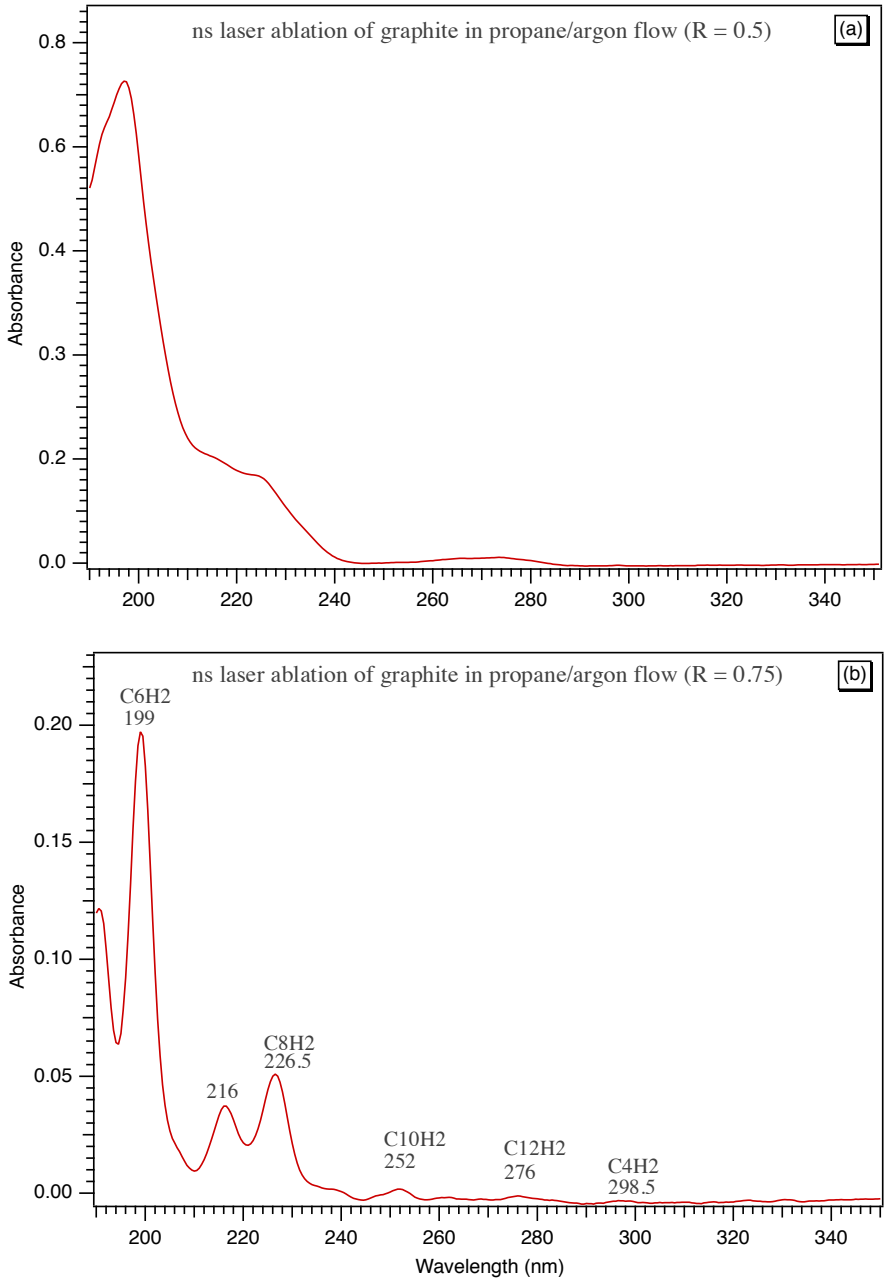

Figure 3.24. UV-Vis absorption spectra of the products resulting from ns laser ablation of graphite in propane/argon gas mixture flow. (a) Propane ratio (R = 0.5). (b) propane ratio R = 0.75. An expanded scale is shown in the indexes for a better view of longer polyynes.

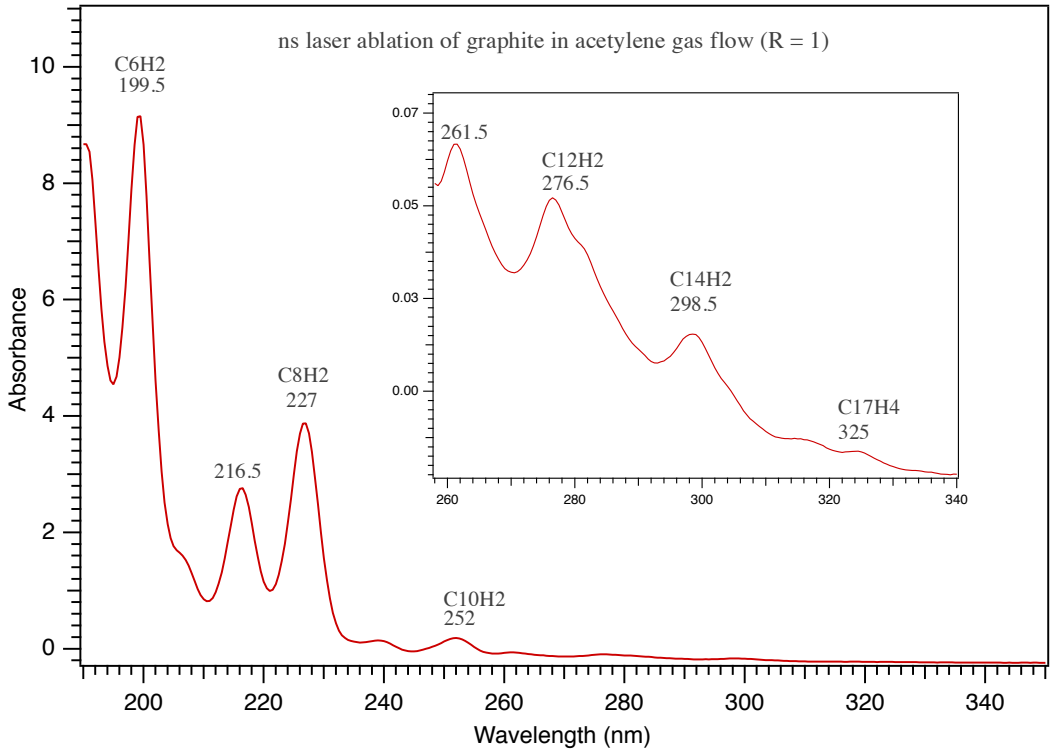

Figure 3.25. UV-Vis absorption spectrum of the products resulted from ns laser ablation of graphite in acetylene gas flow (R = 1). An expanded scale is shown in the indexes for better view of longer polyynes.

The purity of polyynes (χ_p) produced from an experiment can be measured by integrating the ratio of absorbance of polyynes to the unresolved hydrocarbons over the wavelength region from 200 to 400 nm with the aid of the pure polyynes spectra gained from the HPLC. Reference [53] reported that the purity of polyynes synthesized from ns LIB in propane was $\chi_p \cong 0.25$ and from fs LIB also in propane was $\chi_p \cong 0.46$. The purity of the polyynes produced in ethylene in this work was calculated to be $\chi_p \cong 0.46$ from the ns LIB and $\chi_p \cong 0.6$ from the fs LIB. The purity of the polyynes produced from ns LIB in acetylene was calculated to be $\chi_p \cong 0.55$, and a highr value is expected from the fs LIB in acetylene. The fs LIB in acetylene experiment has not been carried out yet.

Although polyyne synthesis experiment results from ns and fs lasers interaction with matter cannot be simply compared since not all the other parameters are the same, it is important to understand how ns and fs laser interact differently with molecules and how the laser wavelength influences the product of an interaction, which could help explain the reason behind the significantly higher polyyne formation rates from ns laser (532 nm) and why purer polyynes are produced from fs laser (800 nm). In a review by [55], ns and fs lasers with very similar focusing conditions were compared. The ns laser only produced neutral fragments, while the parent and many other fragment ions where observed from the fs laser. Depending on the laser wavelength, the ionization efficiency was investigated by [56]. Shorter wavelength should produce more molecular ions since less photon are required for the ionization, the study reported no difference in the molecular ions produced at different wavelengths. Moreover, more fragments were produced at the lower wavelength. This was explained by the larger excess energy at lower wavelength and that a molecular ion can be dissociated by absorbing more photons.

Chapter 4

Conclusion and Recommendations

4.1 Conclusion

Polyyne synthesis is studied in this thesis. Polyynes can be produced by the ns and fs laser interaction with matter in the gaseous, liquid and solid states. fs laser irradiation of organic liquids directly without the aid of carbon particles suspension in the liquid was confirmed to be a successful method to make polyynes. However, the fact that a target molecule has a methyl group does not ensure the formation of methylpolyynes in the product, and the existence of two methyl groups in the target molecule could be the factor that prevented the formation of methylpolyynes. The liquid irradiation is a time consuming experiment compared to LIB and laser ablation of graphite, and LIB can be carried out by bubbling argon in organic liquids or directly in gaseous hydrocarbons with higher polyyne production efficiency from the latter. The yield of longer polyynes produced from fs LIB in ethylene saturates at higher pulse energies, and the yield of longer polyynes produced from ns LIB in acetylene decreases at longer irradiation times. This two observation could be due to the less stability of longer polyynes. The polyyne

production reaction ($C_2H + CH_3C \equiv CH \rightarrow C_4H_2 + CH_3$) was confirmed by the observation of swan bands in the emission spectra of the plasma formed during the LIB.

The Polyyne synthesis experiments carried out in this work in terms of the amount of polyynes produced, can be arranged in the order: ns LIB directly in hydrocarbon gases, fs LIB directly in hydrocarbon gases, ns LIB by bubbling argon in organic liquids, fs LIB by bubbling argon in organic liquids, Laser ablation of graphite in hydrocarbon gas flow, and fs laser irradiation of organic liquids, with ns LIB directly in hydrocarbon gases being the highest and fs laser irradiation of organic liquids being the lowest.

The highest amount of polyynes produced by fs laser was the LIB in ethylene, and the highest amount produced in this study was from the ns LIB in acetylene. Although ns laser produced higher concentration of polyynes, the purity of polyyne produced by the fs laser is significantly higher than those produced by ns laser. This could be due to the simple and very similar molecular structure of ethylene and acetylene.

4.2 Recommendations for future work

- In order to investigate the influence of the starting target molecules in the formation of methylpolyynes or polyynes with end caps other than hydrogen, the production of polyynes from molecules with different functional groups should be studied.
- Further analysis of the irradiation time, pulse energy, pulse length, and gas flow rate dependencies is recommended to better understand the mechanism of polyyne formation.
- Due to the importance of producing polyynes with as high purity as possible, the fs LIB in acetylene needs to be investigated since it's expected to produce highly pure polyynes. Also, other hydrocarbon gases could be studied.
- Setting up an HPLC and standard UV-Vis spectroscopy systems in our lab would improve the efficiency of our polyynes research.
- Surface Enhanced Raman Spectroscopy (SERS) analysis would help in identifying all components in the product even those that cannot be identified with standard UV-Vis spectroscopy because of their limited amounts such as longer polyynes, and components other than polyynes produced in the experiments.

References

[1] Hu, A., Lu, Q. B., Duley, W. W., & Rybachuk, M. (2007). Spectroscopic characterization of carbon chains in nanostructured tetrahedral carbon films synthesized by femtosecond pulsed laser deposition. *The Journal of chemical physics*, *126*(15), 154705.

[2] Shvartsburg, A. A., Hudgins, R. R., Dugourd, P., Gutierrez, R., Frauenheim, T., & Jarrold, M. F. (2000). Observation of "stick" and "handle" intermediates along the fullerene road. *Physical review letters*, *84*(11), 2421.

[3] Kiang, C. H., & Goddard III, W. A. (1996). Polyyne ring nucleus growth model for single-layer carbon nanotubes. *Physical review letters*, *76*(14), 2515.

[4] Kroto, H. W., Heath, J. R., O'Brien, S. C., Curl, R. F., & Smalley, R. E. (1985). C60: Buckminsterfullerene. *Nature*, *318*(6042), 162.

[5] Katz, E. A. (2006). Fullerene thin films as photovoltaic material. In *Nanostructured materials for solar energy conversion* (pp. 361-443).

[6] OSAWA, E. (1970). Superaromaticity. *Kagaku*, *25*, 854-863.

[7] Yadav, J. (2018). Fullerene: Properties, Synthesis and Application. *Research & Reviews: Journal of Physics*, *6*(3), 1-6.

[8] Li, Y., Huang, Y., Du, S., & Liu, R. (2001). Structures and stabilities of C60-rings. *Chemical physics letters*, *335*(5-6), 524-532.

[9] Lu, W., Baek, J. B., & Dai, L. (Eds.). (2015). *Carbon Nanomaterials for Advanced Energy Systems: Advances in Materials Synthesis and Device Applications*. John Wiley & Sons.

[10] Hebard, A. F., Rosseinky, M., Haddon, R., Murphy, D., Glarum, S., Palstra, T., ... & Karton, A. (1991). Potassium-doped c60. *Nature*, *350*, 600-601.

[11] Iijima, S. (1991). Helical microtubules of graphitic carbon. *nature*, *354*(6348), 56.

[12] Yu, M. F., Lourie, O., Dyer, M. J., Moloni, K., Kelly, T. F., & Ruoff, R. S. (2000). Strength and breaking mechanism of multiwalled carbon nanotubes under tensile load. *Science*, *287*(5453), 637-640.

[13] Kelly, B. T. (1981). Physics of graphite.

[14] Yakobson, B. I., Campbell, M. P., Brabec, C. J., & Bernholc, J. (1997). High strain rate fracture and C-chain unraveling in carbon nanotubes. *Computational Materials Science*, *8*(4), 341-348.

[15] Lee, C., Wei, X., Kysar, J. W., & Hone, J. (2008). Measurement of the elastic properties and intrinsic strength of monolayer graphene. *science*, *321*(5887), 385-388.

[16] Pop, E., Mann, D., Wang, Q., Goodson, K., & Dai, H. (2006). Thermal conductance of an individual single-wall carbon nanotube above room temperature. *Nano letters*, *6*(1), 96-100.

[17] Javey, A., Qi, P., Wang, Q., & Dai, H. (2004). Ten-to 50-nm-long quasi-ballistic carbon nanotube devices obtained without complex lithography. *Proceedings of the National Academy of Sciences*, *101*(37), 13408-13410.

[18] Kreupl, F., Graham, A. P., Liebau, M., Duesberg, G. S., Seidel, R., & Unger, E. (2004). International Electron Devices Meeting, IEDM Technical Digest. In *IEEE International* (p. 683).

[19] Pop, E., Mann, D., Reifenberg, J., Goodson, K. E., & Dai, H. J. (2005). International Electron Devices Meeting (IEDM), Washington, DC In *IEEE International* (pp. 253-256).

[20] Hu, X. J., Padilla, A. A., Xu, J., Fisher, T. S., & Goodson, K. E. (2006). 3-omega measurements of vertically oriented carbon nanotubes on silicon. *Journal of Heat Transfer*, *128*(11), 1109-1113.

[21] Nishide, D., Dohi, H., Wakabayashi, T., Nishibori, E., Aoyagi, S., Ishida, M., ... & Shinohara, H. (2006). Single-wall carbon nanotubes encaging linear chain C10H2 polyyne molecules inside. *Chemical physics letters*, *428*(4-6), 356-360.

[22] Smith, B. W., Monthioux, M., & Luzzi, D. E. (1998). Encapsulated C 60 in carbon nanotubes. *Nature*, *396*(6709), 323.

[23] Kataura, H., Maniwa, Y., Kodama, T., Kikuchi, K., Hirahara, K., Suenaga, K., ... & Krätschmer, W. (2001). High-yield fullerene encapsulation in single-wall carbon nanotubes. *Synthetic Metals*, *121*(1-3), 1195-1196.

[24] Bandow, S., Takizawa, M., Hirahara, K., Yudasaka, M., & Iijima, S. (2001). Raman scattering study of double-wall carbon nanotubes derived from the chains of fullerenes in single-wall carbon nanotubes. *Chemical Physics Letters*, *337*(1-3), 48-54.

[25] Hirahara, K., Suenaga, K., Bandow, S., Kato, H., Okazaki, T., Shinohara, H., & Iijima, S. (2000). One-dimensional metallofullerene crystal generated inside single-walled carbon nanotubes. *Physical Review Letters*, *85*(25), 5384.

[26] Suenaga, K., Tence, M., Mory, C., Colliex, C., Kato, H., Okazaki, T., ... & Iijima, S. (2000). Element-selective single atom imaging. *Science*, *290*(5500), 2280-2282.

[27] Okazaki, T., Suenaga, K., Hirahara, K., Bandow, S., Iijima, S., & Shinohara, H. (2001). Real time reaction dynamics in carbon nanotubes. *Journal of the American Chemical Society*, *123*(39), 9673-9674.

[28] Maniwa, Y., Kataura, H., Abe, M., Suzuki, S., Achiba, Y., Kira, H., & Matsuda, K. (2002). Phase transition in confined water inside carbon nanotubes. *Journal of the Physical Society of Japan*, *71*(12), 2863-2866.

[29] Takenobu, T., Takano, T., Shiraishi, M., Murakami, Y., Ata, M., Kataura, H., ... & Iwasa, Y. (2003). Stable and controlled amphoteric doping by encapsulation of organic molecules inside carbon nanotubes. *Nature materials*, *2*(10), 683.

[30] Yanagi, K., Miyata, Y., & Kataura, H. (2006). Highly Stabilized β-Carotene in Carbon Nanotubes. *Advanced Materials*, *18*(4), 437-441.

[31] Li, L. J., Khlobystov, A. N., Wiltshire, J. G., Briggs, G. A. D., & Nicholas, R. J. (2005). Diameter-selective encapsulation of metallocenes in single-walled carbon nanotubes. *Nature materials*, *4*(6), 481.

[32] Kroto, H. (2010). Carbyne and other myths about carbon.

[33] Gibtner, T., Hampel, F., Gisselbrecht, J. P., & Hirsch, A. (2002). End-cap stabilized oligoynes: model compounds for the linear sp carbon allotrope carbyne. *Chemistry–A European Journal*, *8*(2), 408-432.

[34] Lagow, R. J., Kampa, J. J., Wei, H. C., Battle, S. L., Genge, J. W., Laude, D. A., ... & Munson, E. (1995). Synthesis of linear acetylenic carbon: the" sp" carbon allotrope. *Science*, *267*(5196), 362-367.

[35] Sato, Y., Kodama, T., Shiromaru, H., Sanderson, J. H., Fujino, T., Wada, Y., ... & Achiba, Y. (2010). Synthesis of polyyne molecules from hexane by irradiation of intense femtosecond laser pulses. *Carbon*, *48*(5), 1673-1676.

[36] Wakabayashi, T., Murakami, T., Nagayama, H., Nishide, D., Kataura, H., Achiba, Y., ... & Shinohara, H. (2009). Raman spectral features of longer polyynes HC2nH (n=4–8) in SWNTs. *The European Physical Journal D*, *52*(1-3), 79-82.

[37] Ramadhan, A., Wesolowski, M., Wakabayashi, T., Shiromaru, H., Fujino, T., Kodama, T., ... & Sanderson, J. (2017). Synthesis of hydrogen-and methyl-capped long-chain polyynes by intense ultrashort laser pulse irradiation of toluene. *Carbon*, *118*, 680-685.

[38] Liu, M., Artyukhov, V. I., Lee, H., Xu, F., & Yakobson, B. I. (2013). Carbyne from first principles: chain of C atoms, a nanorod or a nanorope. *ACS nano*, *7*(11), 10075-10082.

[39] Hu, A., Sanderson, J., Zaidi, A. A., Wang, C., Zhang, T., Zhou, Y., & Duley, W. W. (2008). Direct synthesis of polyyne molecules in acetone by dissociation using femtosecond laser irradiation. *Carbon*, *46*(13), 1823-1825.

[40] Cataldo, F. (Ed.). (2005). *Polyynes: synthesis, properties, and applications*. CRC Press.

[41] Duley, W. W., & Williams, D. A. (1984). Interstellar polyynes from the disruption of carbon grains. *Monthly Notices of the Royal Astronomical Society*, *211*, 97-103.

[42] Cernicharo, J., Goicoechea, J. R., & Caux, E. (2000). Far-infrared detection of C3 in Sagittarius B2 and IRC+ 10216. *The Astrophysical Journal Letters*, *534*(2), L199.

[43] Maier, J. P., Walker, G. A., & Bohlender, D. A. (2004). On the possible role of carbon chains as carriers of diffuse interstellar bands. *The Astrophysical Journal*, *602*(1), 286.

[44] Eastmond, R., Johnson, T. R., & Walton, D. R. M. (1972). Silylation as a protective method for terminal alkynes in oxidative couplings: A general synthesis of the parent polyynes $H(C{\equiv}C)_nH$ (n= 4–10, 12). *Tetrahedron*, *28*(17), 4601-4616.

[45] Chalifoux, W. A., & Tykwinski, R. R. (2010). Synthesis of polyynes to model the sp-carbon allotrope carbyne. *Nature chemistry*, *2*(11), 967-971.

[46] Taguchi, Y., Endo, H., Abe, Y., Matsumoto, J., Wakabayashi, T., Kodama, T., ... & Shiromaru, H. (2015). Polyyne formation by graphite laser ablation in argon and propane mixed gases. *Carbon*, *94*, 124-128.

[47] Rohlfing, E. A., Cox, D. M., & Kaldor, A. (1984). Production and characterization of supersonic carbon cluster beams. *The Journal of chemical physics*, *81*(7), 3322-3330.

[48] Matsutani, R., Inoue, K., Sanada, T., Wada, N., & Kojima, K. (2012). Preparation of long-chain polyynes of C28H2 and C30H2 by liquid-phase laser ablation. *Journal of Photochemistry and Photobiology A: Chemistry*, *240*, 1-4.

[49] Tsuji, M., Tsuji, T., Kuboyama, S., Yoon, S. H., Korai, Y., Tsujimoto, T., ... & Mochida, I. (2002). Formation of hydrogen-capped polyynes by laser ablation of graphite particles suspended in solution. *Chemical physics letters*, *355*(1-2), 101-108.

[50] Gu, X., Kim, Y. S., Kaiser, R. I., Mebel, A. M., Liang, M. C., & Yung, Y. L. (2009). Chemical dynamics of triacetylene formation and implications to the synthesis of polyynes in Titan's atmosphere. *Proceedings of the National Academy of Sciences*, *106*(38), 16078-16083.

[51] Sun, Y. L., Huang, W. J., & Lee, S. H. (2015). Formation of polyynes C4H2, C6H2, C8H2, and C10H2 from reactions of C2H, C4H, C6H, and C8H radicals with C2H2. *The Journal of Physical Chemistry Letters*, *6*(20), 4117-4122.

[52] Goulay, F., Osborn, D. L., Taatjes, C. A., Zou, P., Meloni, G., & Leone, S. R. (2007). Direct detection of polyynes formation from the reaction of ethynyl radical (C 2 H) with propyne (CH 3–C [triple bond, length as m-dash] CH) and allene (CH 2 [double bond, length as m-dash] C [double bond, length as m-dash] CH 2). *Physical Chemistry Chemical Physics*, *9*(31), 4291-4300.

[53] Taguchi, Y., Endo, H., Kodama, T., Achiba, Y., Shiromaru, H., Wakabayashi, T., ... & Sanderson, J. H. (2017). Polyyne formation by ns and fs laser induced breakdown in hydrocarbon gas flow. *Carbon*, *115*, 169-174.

[54] Wada, Y., Koma, K., Ohnishi, Y., Sasaki, Y., & Wakabayashi, T. (2012). Photoinduced reaction of methylpolyynes H (C≡ C) n CH 3 (n= 5-7) and polyyne H (C≡ C) 5 H with I 2 molecules. *The European Physical Journal D*, *66*(12), 322.

[55] Ledingham, K. W. D., & Singhal, R. P. (1997). High intensity laser mass spectrometry—A review. *International journal of mass spectrometry and ion processes*, *163*(3), 149-168.

[56] Li, A., Imasaka, T., & Imasaka, T. (2018). Optimal Laser Wavelength for Femtosecond Ionization of Polycyclic Aromatic Hydrocarbons and Their Nitrated Compounds in Mass Spectrometry. *Analytical chemistry*, *90*(4), 2963-2969.